2014

GLOBAL ASSESSMENT OF RADIOCARBON ISOTOPIC ANALYSIS FOR PARTICULATE AND DISSOLVED ORGANIC CARBON IN RIVERINE SYSTEMS

Ashley Tucker
Virginia Commonwealth University

GLOBAL ASSESSMENT OF RADIOCARBON ISOTOPIC ANALYSIS FOR PARTICULATE AND DISSOLVED ORGANIC CARBON IN RIVERINE SYSTEMS

A thesis submitted in partial fulfillment of the requirements for the degree of Master of Science at Virginia Commonwealth University

By

Ashley Nicole Tucker
Bachelor of Science
Virginia Commonwealth University, 2011

Major Advisor:
S. LEIGH MCCALLISTER, PH.D.
Associate Professor, Dept. of Biology and Center for Environmental Studies

Virginia Commonwealth University
Richmond, VA
May 2014

ACKNOWLEDGEMENT

I am grateful of my thesis advisor, Dr. S. Leigh McCallister, for the numerous opportunities she provided during my educational experience and the support and encouragement she provided during this study. I would also like to express my appreciation for my committee members, Dr. Vickie Connors and Dr. Scott Neubauer, for their time, patience, and contribution towards the development of this project. I would also like to extend my utmost regard for the VCU Center for Environmental Studies, Dr. Greg Garman, Dr. Clifford Fox and Mrs. Pamela Mason for their guidance and support. To the McCallister Lab members (Lindsey Koren, Rachel Cooper Faison, Eric Hall, Susie Gifford, Arianna Leigh, Thomas Dunlap, and Alyssa Darling), thank you for your camaraderie and insight. For all of the advice, professionally and personally, that helped lead to the success of this project, I am grateful to my colleagues at the Henrico County Central Environmental Lab. To my friends April Herrington, Krystle Simms, and Melanie Rasnic—thank you for understanding while I was gone on writing binges and for not telling me I would never make it. Thank you to my father, Geoff Tucker, for your laughter and your sound advice when I might have gone down a different path. And lastly, to my love and best friend, Kyle Cox—throughout this experience, you reminded me of what I was capable when I had forgotten it myself.

TABLE OF CONTENTS

LIST OF TABLES

Page

LIST OF FIGURES

Page

ABSTRACT

GLOBAL ASSESSMENT OF RADIOCARBON ISOTOPIC ANALYSIS FOR PARTICULATE AND DISSOLVED ORGANIC CARBON IN RIVERINE SYSTEMS

By Ashley Nicole Tucker

A thesis submitted in partial fulfillment of the requirements for the degree of Master of Science at Virginia Commonwealth University

Virginia Commonwealth University, 2014

Major Advisor: Dr. S. Leigh McCallister, Center for Environmental Studies

Rivers are a significant source of particulate and dissolved organic carbon (POC, DOC) into inland waters and coastal systems and provide a fundamental linkage between the terrestrial, oceanic, and atmospheric carbon reservoirs. Recent studies have examined the relationship between the quantity and form (POC vs. DOC) of carbon delivered to the aquatic system; however, little is known about the age of POC and DOC exported and how the radiocarbon age

may vary with latitude, topographic gradient, vegetation, and land use. I provide the first global synthesis of published radiocarbon values of POC and DOC ($\Delta^{14}C$). Inclusion of DOC and POC parameters (μM, $\delta^{13}C$, $\Delta^{14}C$) reveal significant driving forces of DOC (μM), latitude, and elevation (m) as capable of explaining 25% of the variability in $DO^{14}C$ in rivers and POC (μM) and latitude accounting for 15% of the variability in $PO^{14}C$. When $\delta^{13}C$ of DOC and POC and latitude were incorporated with $\Delta^{14}C$ of DOC observations, 61% of the variability in DOC age was explained revealing the necessity to include dissolved and particulate fractions of organic carbon to yield the most robust predictive models. This study found a global trend of increasing age of DOC and increasing $\delta^{13}C$ of DOC and POC with increasing latitude. My study suggests future research should incorporate both particulate and dissolved OC parameters along with elevation, vegetation, land cover, and climate zones to increase understanding of what drives the age of carbon exported in riverine systems.

I. INTRODUCTION

1.1 The Role of Rivers in the Global Carbon Cycle

Rivers, which have historically been viewed as playing an insignificant role in the global carbon cycle, are now recognized as a fundamental linkage between the terrestrial, oceanic, and atmospheric reservoirs (Cole et al., 2007; McCallister and del Giorgio, 2008; Ellis et al., 2012). Through a combination of abiotic and biotic processes, rivers transform and transport a significant amount of particulate and dissolved organic carbon (POC, DOC) from terrestrial environments to coastal seas. Recent studies have estimated that approximately 1 Pg C is exported annually via global rivers to the coastal oceans (Bauer and Bianchi, 2011; Cole et al., 2007; Tranvik et al., 2009; Aufdenkampe et al., 2011). Figure 1A shows the estimated export of carbon between the different major carbon reservoirs in gigatons (Gt) of C yr^{-1}. Initially, the amount of variance seen in estimated river flux of 0.4 to 0.8 Gt of C seems insignificant until the magnitude (approximately half) is compared to the differences in carbon export caused by increased anthropogenic activity via land use change and increased industrial activity. When land use change can alter the flux between the terrestrial and atmospheric reservoirs 1.7 to 1.9 Gt of C yr^{-1}, variances in riverine OC flux of .4 Gt of C yr^{-1} become more significant.

Recent studies have quantified the amount, age and lability of carbon exported along the river continuum (Amon et al., 2012; Butman et al., 2012; Hossler and Bauer, 2012; Moreira-

Turcq et al., 2013). These studies cover a wide range of river system types varying in location (active vs. passive margins), climate, discharge, land cover, soil texture, bedrock lithology, vegetation type, and slope to name a few. Increased anthropogenic activities, including land use change and hydrological accelerations may potentially increase POC and DOC exported from land to aquatic systems. In order to more accurately predict the impact these changes will have on soil and aquatic C budgets, understanding the potential environmental drivers governing the export of variably aged POC and DOC from riverine systems becomes essential.

1.2 Sources of Riverine POC and DOC

Riverine organic carbon (OC) is a heterogeneous mixture comprised of carbon derived from various allocthonous sources (i.e. litter, soil, and marsh-derived organic carbon) and autochthonous sources (i.e. algae, bacteria, and submerged aquatic vegetation). Of the 1 Pg C yr^{-1} that is exported by rivers, approximately half is in the form of POC and DOC with the remainder in the dissolved inorganic pool (Meybeck, 1982; Cole et al., 2007; Bauer and Bianchi, 2011). Both particulate and dissolved organic fractions are derived from distinct organic matter sources (McCallister et al., 2006) and are characterized by different molecular compositions, reactivity, and biogeochemical cycling within aquatic systems (Guo and Macdonald, 2006). In terms of bio-reactivity organic matter may be characterized into three categories of availability (labile, semi-labile, and refractory) based on time scales of utilization. In general, labile organic matter is utilized in a matter of hours to weeks; semi-labile is consumed on a timescale of months to years, and refractory organic matter is metabolized over a timescale centuries to millennia (Davis and Benner, 2007).

1.3 Radiocarbon Isotopic Analysis of Riverine OC

In order to increase understanding of the ways in which OC will become transformed and transported along the river continuum, biogeochemists utilize coupled isotopic analysis ($\delta^{13}C$ and $\Delta^{14}C$) to elucidate both the source and age of OC within riverine systems (Raymond and Bauer, 2001a; McCallister et al., 2004). Stable isotope analysis ($\delta^{13}C$) has proven to be a powerful tool when inferring various sources and pathways of organic matter transformation (McCallister et al., 2006). Because ^{13}C has a higher molecular weight when compared to ^{12}C, fixation of C by various processes such as photosynthesis will result in preferential enrichment of ^{12}C that results in negative ^{13}C values. Because the values will have specific ranges (Figure 1B) based on which carbon source is utilizing inorganic carbon, studies employing ^{13}C can differentiate whether the carbon is sourced from within the system (algal-derived) or whether it is terrestrial in nature (Galy et al., 2008).

During cosmic ray spallation, high energy cosmic rays interact with molecules in the atmosphere, to produce ^{14}C and hydrogen. ^{14}C is a radioactive isotope of carbon, and the amount of radiocarbon of organic matter reflects the ^{14}C content of the atmospheric CO_2 at the time the carbon was fixed. Scientists use radiocarbon dating based on the rate at which cosmogenic ^{14}C radioactively decays (half life 5,730 yr). The term "modern" refers to post-bomb carbon, or carbon considered to be derived from plant sources after 1957 (Evans et al., 2007). Examination of the radiocarbon signature of POC and DOC in natural waters reveals distinct pools which cycle on modern, decadal, and millennial timescales. Because of the spike in atmospheric ^{14}C that occurred following nuclear bomb testing, scientists can utilize the positive $\Delta^{14}C$ values to measure carbon on modern and decadal scales (Figure 1C). Understanding the timescales at which terrestrial carbon cycles within riverine systems helps to identify the links and lags

between terrestrial C fixation and its potential return to the atmosphere via the aquatic system or sequestration in sediments and/or refractory OC pools (Butman et al., 2012; McCallister et al., 2004; McCallister and del Giorgio, 2012). Typically the majority of riverine systems are thought to contain DOC that is dominated by a modern, recently fixed carbon pool (Bauer and Bianchi, 2012; Butman et al., 2012) and a riverine particulate counterpart that is generally older than the dissolved fraction (Rosenheim and Galy, 2012; Rosenheim et al., 2013).

1.4 Potential Driving Factors of the Age of OC Exported from Global Rivers

Researchers have begun characterizing the age of riverine organic carbon with respect to various hydrologic, geomorphic, and climatic controls at both local and regional scales (Hatten et al., 2012; Moyer et al., 2012; Moreira-Turcq et al., 2013). For example, Leithold et al. (2006) concluded that rivers in watersheds containing rapid uplift, steep slopes, and higher levels of erosion were sources of aged POC to the receiving systems. Further, within individual riverine systems, discharge has often been related to the age of POC due to sediment storage processes as well as adsorption and desorption of mineral surfaces that occur within river channels (Goni et al., 2012; Nagao et al,. 2010). Research in the Mississippi/Atchafalaya River system documented an increase in the age POC with increased high-flow events; nevertheless, the age and composition was found to be too variable to elucidate discharge as the sole factor regulating the age of POC in the system, suggesting that multiple factors should be evaluated as potential drivers of riverine POC age (Rosenheim et al., 2013). Although individual studies have investigated potential driving topographic, hydrologic, and biological factors regulating the source and age of POC and DOC in specific riverine systems (Cole and Caraco, 2001; Caraco et al., 2010; Guo and MacDonald, 2006; Hossler and Bauer, 2012), a global study integrating multiple factors on larger scales remains lacking.

1.5 Objectives and Hypothesis

The overall goal of this study was to introduce a global synthesis of published radiocarbon values and their associated $\delta^{13}C$ values of organic carbon from rivers worldwide. From the global synthesis, two research questions were addressed: 1) Are there global trends in the age of particulate and dissolved riverine carbon? 2) Are there relationships between environmental drivers and isotopic patterns that could further elucidate the complex relationships that exist between watershed characteristics and riverine carbon? The first objective was to conduct a global assessment of published $\Delta^{14}C$ data of riverine POC and DOC to evaluate a potential relationship between the radiocarbon age of carbon as a function of latitude. I hypothesized as proximity to the North Pole increased, a global trend in the age of radiocarbon POC and DOC would increase. The second objective of the study was to employ geospatial tools to couple the radiocarbon age of POC and DOC with pre-existing topographic databases in order to identify driving environmental factors. I hypothesized that elevation and slope would show the strongest relationship with $\Delta^{14}C$ of POC and DOC showing increased elevation and slope would be tied to increased radiocarbon ages. Additionally, I expected increased discharge and high-flow events to result in increased ages of radiocarbon POC and DOC. I also hypothesized land use cover would yield a significant relationship with the reported radiocarbon riverine values of POC and DOC primarily driven by changes in the level of perturbation occurring. Lastly, I expected vegetation to show a significant relationship with the radiocarbon age of POC and DOC via the $\delta^{13}C$ signatures associated with various types of vegetation.

II. METHODS

To answer the research questions, an extensive review of literature and databases was performed and added to other topographic databases to assess potential global trends. In order to organize the research, selection criteria for locations to be used in this study were established based on how to best characterize the interactions on a broad scale that was appropriate for the amount observations and also excluded systems with vastly different transformation patheways. After the literature review was compiled, the data was added to other current databases containing topographic information in order to conduct geospatial analysis. Linear regressions and multivariate regressions were utilized to elucidate relationships that existed between the age of OC in rivers and the environmental factors examined. Additionally, the age of OC for the classes within the categorical data were examined to determine global trends.

2.1 Selection Criteria

An extensive review of peer-reviewed publications, conference presentations, and research group databases was conducted. Published radiocarbon carbon ages and associated $\delta^{13}C$ values of riverine POC and DOC were collected up to January 2013. While streams are considered inland systems and are a part of the river continuum, these data were not included in this study in order to focus the research on larger drainage systems. Additionally, the transport and transformation of OC in brackish and saltwater systems is very different from freshwater systems, thus POC and DOC data compiled from systems with salinity greater than 2 practical salinity units (PSU), were not included excluding estuaries and other coastal systems. A little more than half (270) of the

radiocarbon measurements were collected between 1972 and 2005. Two hundred twenty-five observations were made from 2005 to 2009, indicating that this field has grown rapidly in recent years. Data were reported in $\Delta^{14}C$ (‰), Fm (fraction modern), and conventional radiocarbon age. To relate all three variable, the more depleted (or more negative) the $\Delta^{14}C$ (‰), the further below 1.000 Fm becomes and the older the age becomes. Additionally, not all observations took into account the year that modern, or post-bomb carbon appeared. Overall, general themes impacting isotopic patterns of riverine organic carbon within the literature were elevation, discharge, vegetation, land use change, geologic processes, and seasonality.

2.2 Geospatial Analysis

This study utilized the analysis tools of ArcMap 10.1 using the World Geodetic System – 1984 (WGS 84) geospatial coordinate system. The use of this coordinate system was necessary in order to include a z-axis component to the data for analysis of elevation and slope data. Furthermore, this projection shows a relatively unskewed and effective visual display of the entire globe. A global shapefile acquired from the Global Runoff Data Center was included for boundaries for the continents and locations of global rivers.

Riverine POC and DOC radiocarbon data was imported in ArcMap using the x,y coordinate system with longitude defined as “x” and latitude as “y”. Once the table was created, the x,y coordinate data was added to the database as a shapefile layer. This allowed for the observations to become geospatially referenced. Because of the variances in how latitude and longitude can be calculated and reported, the data points were joined to the global shapefile and buffered to two degrees (Figure 2A). This buffered shapefile, a means of capturing data within a specified area of the data points, was used throughout the geospatial analysis in order to capture the general factors of the area sampled due to discontinuity of reported topographical and

hydrologic data (Butman et al., 2012). Frequencies in sampling sites were characterized by circle size with larger circles indicating systems with relatively higher numbers of observations (Figure 2B).

Global elevation data were retrieved from the United States Geological Survey (USGS) using the GTOPO30 elevation model with a 30 arc-second grid, meaning within each raster or rectangular pixel, the grid is equal to approximately 1 kilometer at the equator (Danielson and Gesch 2008). From these raster data, the spatial tool "slope" was used to evaluate the rate of change in elevation for each data point (Figure 3).

Land use data from the Food and Agriculture Organization of the United Nations (FAO) was used in an effort to characterize land use patterns. The FAO provides a database of world land use into 11 categories based on land cultivation and forest or urban presence (Figure 4). This database reports dominant land cover patterns referred to as Global Agro-Ecological Zones (GAEZ). This study utilized GAEZ v3.0 that provided raster data at a 30 arc-second resolution.

Vegetation data were collected from the Goddard Institute for Space Studies from a database that provides a high-resolution database of global vegetation and land use. The data source reports vegetation data from over 100 published sources that collapses 180 vegetation types into 32 major global categories (Figure 5). This data set reports each grid at a 1x1 degree latitude and longitude resolution. Once these layers were added to ArcMap, they were joined to the buffered data points and clipped to allow for ease of analysis

Climate zones categories were also established to determine if relationships existed between the age of DOC and POC in climates with roughly estimated similar characteristics.

These categories were defined as Boreal/Arctic (latitudes greater than 55°), Temperate (latitudes between 55° and 23°), and Tropical (less than 23°).

2.3 STATISTICS

Using the Zonal Statistics tool in ArcGIS, summary statistics were calculated for elevation, slope, vegetation, and land cover. From there, average elevation, slope, most dominant vegetation, and land cover were extrapolated to the observations collected during the review. Using these results as well as the compiled data, relationships among the dependent variables, ($DO^{14}C$ and $PO^{14}C$), and the remaining factors were examined. For variables with non-normal distribution, natural log transformations on the conventional radiocarbon age were performed in order to move these variables towards normality. In the presence of negative values (as these logs are undefined), a constant value was added in order to perform the transformations. This method has been shown to provide a new value that does not alter the resulting relationships between variables (Barros et al., 2011). Outliers were removed per the outlier labeling rule and a normal distribution of the dependent variables was generated. Individual linear regressions were performed to determine significant relationships (α=0.05). Stepwise multivariate regressions were utilized with the statistical package allowing only variables with statistically significant p-values (significance level of $\alpha = 0.05$). In each of the models, predicted values for the natural log age of organic carbon were defined by the following equation:

$$[1] \qquad Y = B_{0+}B_1X_1 + \ldots + B_nX_n$$

where X_n represents each predictor variable and B_n is the corresponding coefficient. Individual scatter plots were created to assess the validity of the modeled outputs. Individual $DO^{14}C$ and $PO^{14}C$ observations were plotted against predicted $DO^{14}C$ and $PO^{14}C$ outcomes and normal

probability plots and variance of the residuals were examined to determine the behavior of the multivariate regression.

In order to assess the potential impacts that the categorical data (land cover, vegetation, and climate zone) may have had on the natural log age of DOC and natural log age of POC trends, one-way analysis of variance (ANOVA) tests were run at a significance level of $\alpha=0.05$. Post Hoc Tukey Honestly Significant Difference Tests (HSD) were conducted to tease apart significant differences between the categories for each group ($\alpha=0.05$). For ease of statistical analysis, the categories for land cover were grouped into 6 different classes based on which type was most heavily prevalent: cultivated, forested, grass and woodland, built-up, mixed, and barren/water. Additionally, the vegetation data were further condensed into 6 categories based on a simple classification logic published by Running et al. 1995; evergreen needle leaf, evergreen broadleaf, deciduous mixed, grasses, tundra, and desert, ice, or cultivation (Table 1). All statistical analysis was performed using the statistical package IBM SPSS Statistics 21.

III. RESULTS

3.1 General Description of Riverine Systems

My study examined 63 individual riverine systems (Table 2) with a total of 572 individual observations pulled from 47 different publications and online databases ranging from published dates of 1981 to 2013. Figure 2A shows riverine locations studied ranged from -38.7° S to 70.8° N representing locations on all continents with the exception of Antarctica. In general, the most well-studied region of this data set was the Arctic encompassing the Lena, Ob', Mackenzie, Yukon, Kolyma, and Yenisey rivers (Figure 2B) as provided by the PARTNERS research effort with 20 $PO^{14}C$ observations and 110 $DO^{14}C$ measurements. In addition, significant research efforts have focused on assessing the $DO^{14}C$ and $PO^{14}C$ along the eastern coast of North America and the Mississippi River. In the Southern Hemisphere, the Amazon is the most well-studied riverine system with 31 $PO^{14}C$ and 33 $DO^{14}C$ observations reported from five different studies.

The mean elevation of the systems studied was 224 ± 525 meters, ranging from sea level to locations as high as 4400 meters above sea level. The highest elevations were reported along the Amazon (Brazil), the Liwu River (Taiwain), and the River Congo (Congo). The lowest elevations were associated with the Langyang His (Taiwain), the Parker (USA), and the Atchafalaya (USA). Slope values ranged from 0.001% to 2.65 % with the mean slope of 0.248% ± 0.394%. The Narayani and Kosi Rivers in India and points along the Amazon had the highest slopes (greater than 2.00) in this study. The lowest slope values were found at points along the

floodplains of the Amazon in addition to the Ganges (India), Parker (USA), Rio Grande (USA), and Rio Negro (Brazil)—all with slope values <0.01.

The most prevalent land cover type was land that was mostly forested. Land cover was analyzed for mean values of $\delta^{13}C$ and $\Delta^{14}C$ of DOC and POC within each of the groups (Table 3). The most depleted average $\delta^{13}C$ for DOC and POC occurred in the barren group (-29.2 ± .2 ‰) and the mixed group (-28.4 ± 3.5 ‰), respectively. The most enriched average $\delta^{13}C$ values occurred in grass and woodlands ($DO^{13}C$ = -25.3 ± 1.9 ‰) and mostly cultivated lands ($PO^{13}C$ = -25.2 ± 2.0 ‰). The oldest average DOC was found in cultivated land (-60 ± 139 ‰) and the youngest average DOC was seen in mostly barren land (216 ± 107 ‰). The oldest POC on average was found in cultivated land ($PO^{14}C$ = -351 ± 283 ‰) and the youngest average POC was found in mostly built up land ($PO^{14}C$ = -72 ± 31 ‰) (Table 3).

The dominant vegetation type was deciduous mixed vegetation including deciduous forest, woodland, and shrubland (Table 3). The means of $\delta^{13}C$ (‰) and $\Delta^{14}C$ (‰) within each group generally followed expected trends in latitude reflecting the associated differences in climate. The most enriched average $\delta^{13}C$ signatures were seen in grasses ($DO^{13}C$ = -24.9 ± 2.1 ‰) and evergreen needleleaf ($PO^{13}C$ = -25.7 ± 2.9 ‰). Table 3 shows that the most depleted $\delta^{13}C$ signatures were found primarily in regions populated with evergreen broadleaf vegetation ($DO^{13}C$ = -27.7 ± 2.3 ‰) and tundra ($PO^{13}C$ = -28.5 ± 2.6 ‰). The most enriched average $\Delta^{14}C$ of DOC in rivers was found in regions with primarily evergreen broadleaf vegetation (113 ± 137 ‰) while the most enriched average riverine $\Delta^{14}C$ of POC was seen in regions dominated by evergreen needleleaf (-158 ± 206). Table 3 also shows the most depleted riverine $\Delta^{14}C$ DOC and POC occurred in the tundra (-52 ± 130 ‰ and -424 ± 92 ‰, respectively) (Table 3).

3.2 Riverine DOC Concentrations and Stable and Radiocarbon Dynamics

DOC concentrations ranged from 14.2 μM to 2825.0 μM with a mean of 459.2 ± 329.2 μM (Table 4). The Pozuzo River (Amazon) and the Yukon River (Arctic) were the lowest and highest observed DOC concentrations, (14.2 μM and 2825.0 μM, respectively) (Table 2). In contrast, $DO^{13}C$ observations were more centered around the mean of -27.0 ± 2.1 ‰ with a more narrow range of -32.4 ‰ (Potomac River, USA) to -18.0 ‰ (Delaware River, USA) (Table 4). A total of 275 individual observations of $DO^{14}C$ were included in the data set and ranged from -463 ‰ to 383 ‰ or from 4890 years to modern age C with a mean value of 22.15 ± 114 ‰. The variability in DOC age between and within individual systems is shown in Figures 6A and 7. Further it is noted that overall riverine $DO^{14}C$ tends to be more modern than its particulate counterpart (Figure 7). In general, riverine $DO^{14}C$ varied more between systems than within an individual system (Figure 8A). The minimum $DO^{14}C$ value, or oldest observed C, was measured in the Sagavanirktok River in the Arctic; conversely, the maximum value, or most enriched $\Delta^{14}C$ of DOC, was located in the Sacramento River, California (Table 2). The Obidos River (Amazon) was the youngest, or most modern of the riverine systems sampled, with an average of 265‰, and the oldest riverine system in terms of DOC age was the Sagavanirktok (Arctic) with a $DO^{14}C$ average of -352.5 ‰ (3400 yrs).

The $DO^{14}C$ data was skewed and a natural log transformation of the age of the DOC was carried out in order to perform parametric statistical tests. A correlation matrix showed $DO^{13}C$ (‰), latitude, and average elevation to have positive correlations and DOC (μM) to have a negative correlation with the age of DOC. Individual linear regressions between the radiocarbon age of DOC and each significant variable were performed (Figure 9A-C, Figure 10 A-C). $DO^{13}C$ (‰) was negatively related to the age of DOC ($R^2 = 0.079$; $p < 0.001$; $n = 258$) (Table 5, Figure

9B). Latitude showed a weak relationship with the radiocarbon age DOC (R^2 =0 .017; p = 0.013) (Table 5) but evaluation of the DOC radiocarbon age in each climatic zone yielded significantly stronger individual regressions within the groups with the tropical zone showing the most powerful correlation (R^2 = 0.367; p<0.001) (Figure 11). A stepwise multivariate linear regression was performed incorporating DOC (μM), latitude, and elevation based on the statistical software determination of significance (Table 6) that accounted for approximately 25% of the variability seen in the radiocarbon age of DOC observations (Adj. R^2 = 0.249; p < 0.001; n = 176) (Table 7). This multivariate linear regression, referred to as MLR $DO^{14}C$, found DOC concentration to be a negative driver of radiocarbon age while both latitude and average elevation had a positive influence on the associated DOC age (Table 7). Residual normality plot revealed the residuals were normally distributed however there was slight homogeneity in the plotted variance of the residuals.

3.3 Riverine POC Concentrations and Stable and Radiocarbon Dynamics

POC concentrations ranged from a minimum of 5.9 μM in the Mackenzie River (Arctic) to a maximum of 20200 μM in the LiWu River (Taiwan) and had a mean of 687.7 ± 2520.0 μM. A considerably larger range is seen in POC concentrations (Table 2). $PO^{13}C$ values ranged from -38.0 in the Ob River (Arctic) to -17.0 along the Rio Fajardo (Puerto Rico) with a mean of -27.5 ± 3.0. A total of 297 individual riverine $PO^{14}C$ observations were compiled in with values ranging from -957 ‰ (roughly 24,000 yrs) to 142 ‰ (modern C), located in the LiWu River (Taiwan) and in the Amazon watershed, respectively (Table 2, Table 4). The mean of the riverine POC radiocarbon values was -204 ± 213 ‰, (1800 yrs); however, there was a large variability in radiocarbon ages both within and between systems suggesting significant temporal and spatial changes (Figure 6B). The mean $PO^{14}C$ values for each riverine system included in

this study are seen in Figure 7. The river system with the most modern POC was the Amazon (142 ‰); conversely, the oldest observations on average were observed in samples collected along the LiWu River (-835 ‰), or ~ 14100 yBP (Table 2 and Figure 7).

Similar to the $DO^{14}C$ data, the $PO^{14}C$ dataset was skewed and a natural log transformation was applied to the data in order to run parametric statistics. A correlation matrix for the radiocarbon age of POC was created and $PO^{13}C$ (‰) ($r = 0.230$), and latitude ($r = 0.255$) (Table 5) were determined to be the significant correlations. Linear regressions were run between the radiocarbon age of POC and POC concentration and $PO^{13}C$ (Figure 12A and12B, respectively). Of the two, only $PO^{13}C$ was found to have a significant relationship but weak negative correlation with the radiocarbon age ($R^2 = 0.048$; $p = 0.001$) (Figure 12B). Globally, there was no significant relationship between the POC radiocarbon age and latitude (Figure 13). However, when riverine systems were grouped into climate zones, there were both strong negative and positive correlations with latitude. Particulate samples from rivers located in the boreal/arctic zone showed a strong negative correlation ($R^2=0.767$; $p<0.001$) with latitude indicating that as one moves poleward, the age of the riverine POC increases (Figure 13). Rivers with observations located in New Zealand (near 40°S) were not included in the temperate regression because of the major differences that exist for those systems that differ from other temperate systems. POC samples from the temperate zone showed a slightly weaker but significant positive correlations ($R^2=0.279$; $p<0.001$), and the tropical zone showed no significant relationship ($R^2 =0.046$; $p<0.001$). Lastly, a stepwise multivariate regression was performed, (referred to as MLR $PO^{14}C$), to assess the influence of POC concentration, $PO^{13}C$, and latitude on the age of riverine POC. MLR $PO^{14}C$ found POC concentration and latitude to be statistically significant driving variables of global riverine POC age with slight positive

coefficients of 4.7E5 and 0.007, respectively (Table 6). This multivariate regression was able to account for approximately 15% of the variation seen in global riverine radiocarbon POC ages (Adj. R^2=0.151; p<0.001; n=112) (Table 7). MLR $PO^{14}C$ behaved poorly when compared to MLR $DO^{14}C$ as the predictions were not normally distributed and there was less variance in the predicted residuals.

3.4 Linkages Between the Radiocarbon Age of POC and DOC

A correlation matrix incorporating both dissolved and particulate OC parameters was created and showed significant, positive correlations between the radiocarbon age of DOC and the 5 following variables: $DO^{13}C$ (r = 0.433), the $PO^{14}C$ age (r = 0.277), POC (μM) (r =0.277), $PO^{13}C$ (r = 0.486) and latitude (r = 0.487) (Table 5). Linear regressions between $DO^{14}C$ and each statistically significant correlation variable were run (Figure 9A-C, Figure 10A-C). The most robust relationship existed between the $DO^{14}C$ and $PO^{14}C$ observations (R^2 = 0.256; p < 0.001; n = 107) (Table 5, Figure 10C) with DOC aging concomitantly with POC. The most robust predictive multivariate regression existed when all of the independent variables potentially impacting $DO^{14}C$ were examined with the inclusion of the POC, $PO^{13}C$, and $PO^{14}C$ data as well. The statistically significant regression showed $DO^{13}C$, $PO^{13}C$, and latitude to be statistically independent positive coefficients impacting the age of DOC found in global rivers (Table 6). This regression (MLR $DO^{14}C/PO^{14}C$) was able to account for approximately 61% of the variance in the radiocarbon age of DOC (Adj. R^2=.607; p<0.01; n=43) (Table 7). This was the most well-behaved MLR of the study when both $DO^{14}C$ and $PO^{14}C$ parameters were included.

3.5 Land Cover, Vegetation and Climate Zone Influence on The Radiocarbon age of POC and DOC

A simple one-way ANOVA was conducted to compare the effect of land cover and vegetation type on the radiocarbon age of DOC and POC (Table 3). The mean radiocarbon age of DOC from rivers draining barren land cover, (216 ‰, or modern) was significantly younger than DOC from rivers in all the other land cover groups with the exception of forested land (59 ‰, or modern) (Table 3). Additionally, POC from rivers located in land classified as cultivated was significantly older than built-up land type (~2900 years and 500 years, respectively) (Tables 3, Table 8A). Significant differences were found between the radiocarbon age of riverine DOC derived from the various vegetation groups with the DOC from areas with evergreen broadleaf vegetation having the most modern radiocarbon age (Tables 3 and 8B). Similar to the DOC results, the radiocarbon age of POC from rivers dominated by varying vegetation groups were significantly different. POC from rivers within the tundra category were significantly older (~4300 years) than all of the other categories with the exception of the grasses group. Riverine POC from the grasses group was only significantly older (~2300 years) than that derived from rivers draining land classified as evergreen needleleaf (Table 8B). Lastly, significant differences in the age of riverine DOC and POC existed across three broad climatic groups: boreal/arctic, temperate and tropical (Table 3 and Table 8C). The age of riverine DOC was significantly different across the entire climatic gradient, whereas the POC was similar between the temperate and tropical climatic zones and significantly older in the boreal/arctic (~3400 years).

IV. DISCUSSION

4.1 Environmental Drivers of the Radiocarbon Age of Riverine DOC

One of the most fundamental questions asked in my study is whether different topographic, hydrologic, and biological variations can drive the observed patterns in global $DO^{14}C$ values in riverine systems. Collectively, riverine DOC concentration, latitude, and average elevation are the primary variables influencing the associated DOC age (Table 7). The correlation between DOC concentration and age derived from MLR $DO^{14}C$ reveals a global trend of younger, $\Delta^{14}C$ enriched DOC with increasing DOC concentrations and is supported by local or regional studies which suggest the DOC pool is dominated by modern carbon (Benner et al., 2004; Evans et al., 2007; Raymond et al., 2007).

MLR $DO^{14}C$ also suggested a relationship between river system elevation and the age of DOC in the system such that increases in elevation yielded more highly aged DOC. This may result from a greater tie between higher elevation aquatic systems and their surrounding watershed, thus linking the aquatic processes in these systems more tightly to terrestrial C dynamics (Lapierre and del Giorgio, 2012). In addition, recent studies have characterized the transport of aged C along small mountainous rivers and near active tectonic plates (Moyer et al., 2012; Galy et al., 2007). The transport of aged DOC at sites such generally high elevation may account for the trend of older DOC with increased elevation.

4.2 Environmental Drivers of the Radiocarbon Age of Riverine POC

My data suggest globally, that when other variables are included, the amount of POC in as these with the riverine water column influences its bulk radiocarbon age. Examined together with no other variables, a relationship was not seen; however, when including other factors (MLR $PO^{14}C$), a relationship does seem to exist. In the past, a regional-scale relationship between POC concentration and age had been reported; my results are suggestive that a global-scale relationship may also exist (Wei et al., 2010; Leithold et al., 2006). Further, the radiocarbon age of riverine POC increases as the ^{13}C signature becomes less depleted (Figure 12B). Typically, $\delta^{13}C$ of POC from river systems is more depleted than its marine counterpart with values ranging from -24‰ to -31‰. More enriched $PO^{13}C$ were observed in several riverine systems whose vegetation was dominated by C4 grasses. The older aged POC associated with more enriched $\delta^{13}C$ may be a result of soil C dynamics that are unique to these regions. Alternatively, the trend of younger POC associated with more depleted $\delta^{13}C$ may be a result of increased algal contributions to the POC pool as these tend be both more negative and modern (McCallister and del Giorgio, 2012). Lastly, the more δ^{13-}enriched and older POC may also be a result of degradation by the microbial community as they are thought to prefer more labile, or younger, carbon sources (Bianchi and Bauer, 2011). Greater isotopic analysis of C including $\delta^{13}C$ of PIC would help elucidate the source of POC (autochthonous, allochthonous) and whether the terrestrial contributions are derived from C enriched soils or from geologic processes such as sediment erosion and mineral weathering (Bianchi and Bauer, 2011; Hossler and Bauer, 2012; Mayorga et al., 2005; Moreira-Turcq et al., 2013; Rosenheim et al., 2013).

The radiocarbon age of POC is also tied to the regional vegetative cover with the oldest average POC found in boreal tundra regions and the youngest derived from areas comprised

primarily of evergreen needleleaf vegetation, typical of tropical climates (Table 3). This is not surprising as tundra soil C stocks are typically ancient having accumulated over centuries whereas, tropical soils tend to be comprised of rapidly recycled modern organic material (Trumbore 2000; Mayorga et al., 2005). The export of this carbon into the riverine environment is controlled by local soil and hydrological processes.

4.3 Coupling Dissolved and Particulate Carbon Observations

The biotic and abiotic transformation of POC into DOC via the microbial loop and other physicochemical processes is critical to carbon dynamics in lotic systems (Bianchi and Bauer, 2011). Despite the obvious linkages between the two organic matter pools, many studies, particularly of radiocarbon analysis have suggested that the two pools are isotopically distinct and cycle independently (Raymond and Bauer 2001b; Raymond et al., 2004; Bianchi and Bauer, 2011). The conclusion that the radiocarbon ages of riverine dissolved and particulate organic matter are uncoupled may be the result of limited data as these studies have typically been conducted on a local basis. My data suggest that there are similarities in global patterns of $PO^{14}C$ and $DO^{14}C$. For example the $\delta^{13}C$ signatures of both DOC and POC became more enriched with radiocarbon age (Figure 9B, 12B) suggesting either similar source inputs or OM transformations. Linkages between the $\delta^{13}C$ of POC and its corresponding radiocarbon age have been described before by Galy et al. (2008) for rivers within the Brahmaputra River basin and suggest that the heaver $\delta^{13}C$ values in systems with lower concentrations of OC could indicate greater contribution from allochthonous pre-aged organic matter. Further Bauer and Bianchi (2011) suggested that microbial decompositional preferences for vascular plant material versus algal and bacterial detritus may shift the overall $\delta^{13}C$ enrichment of the system. However, the strongest linkage between the sources and cycling of DOC and POC in riverine systems is the highly

significant regression of their ages (R^2=0.256; p<0.001; Figure 10C). To date this is the only study to suggest such a relationship on a global scale.

4.4 Global Trends in the Radiocarbon Age of Riverine DOC and POC

A coupling of DOC and POC observations revealed the most robust predictive relationship (MLR $DO^{14}C/PO^{14}C$, Figure 14C) with approximately 61% of the variation in riverine $DO^{14}C$ attributed to changes in $DO^{13}C$, $PO^{13}C$, and latitude. Overall, global trends in increased DOC age in riverine systems as one moved towards the North Pole and as $DO^{13}C$ and $PO^{13}C$ became concurrently more enriched (Table 7). The system-wide enrichment of $\delta^{13}C$ DOC as the age of riverine DOC increases is likely a result of increased algal production occurring simultaneously with bacterial utilization and preference for modern C (Raymond and Bauer, 2001b). This observed pattern might also explain the relationship between older DOC located in systems with generally lower DOC concentrations. In a study on soil carbon dynamics, Trumbore (2000) characterized an increase in the age of carbon found in soils along a tropical to boreal gradient—a finding that could be strongly tied to increased ages of both DOC and POC as boreal and arctic soils contain large reservoirs of carbon which have accumulated over centuries (Hobbie et al., 2000). There has been increasing concern that this soil reservoir has become destabilized as a result of warming temperatures and increased hydrology and is exporting growing amounts of pre-aged POC and DOC to the adjacent river systems (Raymond et al., 2007; Guo et al., 2007).

4.5 Local and Regional Observations versus Global Trends

This study has described global trends in riverine POC and DOC radiocarbon age that has previously only been characterized on a local or regional scale. These findings add to the growing body of literature which suggests that radiocarbon ages of dissolved and particulate

carbon may increase our understanding of the factors influencing riverine biogeochemical carbon cycling (Caraco et al., 2010; Cole and Caraco 2001; Guo and MacDonald, 2006; Hossler and Bauer, 2010; McCallister et al., 2004; Raymond and Bauer, 2001b). Moreover, the correlations established between riverine OC and elevation, slope, land cover, and vegetation become informative when coupled with trends seen on local and regional scales. For example riverine carbon isotopic composition at regional scales show marked differences with discharge, (Raymond and Bauer, 2001b) whereas this factor is less significant at global scales. Regional trends with increasing proximity to the North Pole within the three climate zones (Figure 11) revealed generally decreasing age of DOC in tropical latitudes and a general increase in age in temperate and boreal/arctic zones. Most likely, the latitudinal variations in the tropical zone are driven by system specific local factors such as steep slopes or active margins with seismic uplift that produced pre-aged carbon from bedrock and minerals (Leithold et al., 2006; Hilton et al., 2010). POC, on the other hand, showed a decrease in age with latitude for the boreal region but increased in age in both the tropical and temperate zones (Figure 13). While the increasing POC age in boreal systems with latitude is consistent with increased permafrost reservoirs, the trends in the tropical and temperate zone are less straightforward. Potentially they may be related to soil C dynamics in these areas or other driving factors.

One factor which I believe is confounding my interpretation is elevation. The strength of the relationship between elevation and the age of OC found in rivers may have been stronger if more $\Delta^{14}C$ observations had included elevation of the sampling site. If, as hypothesized, systems at higher elevation are more closely tied to the soil C processes that occur in their surrounding watersheds (Lapierre and del Giorgio, 2012), the potential relationship of elevation older OC in rivers may have been masked by the extrapolated averages for the sites that had to

be derived using zonal statistics in GIS. When generally higher elevations were examined on regional scales, we see trends in young soil in low latitudes (Amazon) and older soil in high latitudes (Yukon) (Figure 15A). Also, such close coupling of elevation with land use change may be why the relationship between elevation and $PO^{14}C$ was difficult to extrapolate on a global scale. When specific average elevation was provided in publications used in the literature review, that value was compared to the average elevation generated by ArcGIS zonal statistics. Every point available generated by the Zonal Statistics tool, was lower than the actual average elevation. Further, the slope values were calculated from derived elevation and may be why a statistically significant relationship between slope and $PO^{14}C$ and $DO^{14}C$ was not found. When examining observations on a regional scale, we see that systems with the highest slope gradients contain the oldest observations of $\Delta^{14}C$ along the LiWu River (Hilton et al., 2010) yet additional systems with steep slopes had $\Delta^{14}C$ values that were not nearly as aged (Figure 15B). Conversely, we see the lowest slope values associated with modern C in the floodplains of Amazon (Mayorga et al., 2005). Future investigations into watershed relief may help better resolve the relationship between riverine organic matter age and elevation and slope.

Although categorical data were not included in the multivariate regressions, there were significant relationships when comparing the mean ages of DOC and POC within the groups. In mostly barren land, the $\delta^{13}C$ of DOC was the most depleted and was also the youngest DOC suggesting these systems on average are comprised of recently fixed algal C. The tundra vegetation group which is typical of a boreal climate with large stores of permafrost had the oldest Δ^{14} DOC, POC observations (- 52 ‰ $\pm$ 130 and -424‰ $\pm$ 92, respectively, Table 3). In addition, the DOC derived from evergreen broadleaf dominated systems was significantly younger than every other vegetation class that could be attributed to modern rapidly cycling soil

organic material typical of warmer, low latitude climates (Table 3) (Trumbore, 2000; Bonan et al., 2003). Lastly, the oldest DOC and POC was located in mostly cultivated lands suggesting that perturbations from agricultural activity may in fact be releasing old, refractory carbon to the riverine system in both particulate and dissolved form (Table 3).

Land cover as a driver of riverine radiocarbon POC and DOC age may be related more to the changes in land cover as vegetation decreases and the system moves towards increased agriculture and urbanization. Understanding whether terrestrial systems are experiencing destabilization of previously stored and sequestered soil C is essential in order to decrease major uncertainties that exist in climate change forecasts (Evans et al., 2007). Examining the age of C in the receiving riverine systems may help to alleviate some of this uncertainty. Soil destabilization may occur when the land cover and natural vegetation is altered through anthropogenic activities, be it through urban/industrial development, agricultural growth, or warming of permafrost (Sickman et al., 2010; Gu et al., 2011; Evans et al., 2007; Amon et al., 2012). Urban and industrial development was examined along the Yellow River in China, where profound land use change has been characterized (Gu et al., 2011). Impacts on the Yellow River due to these changes could have significant influences on the biogeochemical cycling of C where the source and age of the OC pool is just now being characterized (Wang et al., 2012). Furthermore, Sickman et al. (2010) reported land use change along the Sacramento-San Juaquin River basin was tied to continued export of aged carbon decades after the land conversion processes were complete. Moreover, Moyer et al. (2012) showed that rivers located near agricultural land and irrigation canals exported significantly aged DOC. In Butman et al. (2012), they utilized $DO^{14}C$ measurements of 15 river basins in the United States to show that systems with higher discharge, comparatively greater vegetation cover, and lower population density

tended to export relatively modern DOC. These studies showed increased anthropogenic activity and decreased water flow are associated with older organic carbon export.

Many studies suggest differences in organic matter ^{13}C and ^{14}C signatures on local and regional scales when differences in discharge and precipitation occur (Butman et al., 2010; Nagao et al., 2010; Rosenheim et al., 2013). However, the influence of discharge on a global scale may be difficult to tease apart as the watershed basins vary so drastically (Butman et al., 2010) and often sampling occurs at single intervals without seasonal and temporal coverage (Alin et al., 2008; Amon et al., 2012; Aramaki et al., 2010; Ellis et al., 2012; Hélie and Hillaire-Marcel, 2006; Masiello and Druffel, 2001; Moreira-Turcq et al., 2013; Townsend-Small et al., 2007). While capturing the biogeochemical processes that occur during high-flow versus low-flow periods and summer versus winter flows are essential to understanding the eventual fate of terrestrial C in riverine systems, a more uniform approach to reporting seasonality and discharge from future studies could help establish global baseline trends that could further our understanding of the age of terrestrial OC exported to riverine systems (Spencer et al., 2012).

4.6 Conclusions

Recently, an increasing number of studies detailing the age of POC and DOC exported from multiple rivers suggests a growing area of research which attempts to bridge the gap between terrestrial and aquatic biomes and identify the source and fate of terrestrial organic carbon in aquatic systems. In order to elucidate relationships between the radiocarbon age of POC and DOC and potential driving environmental and topographic factors, a global synthesis was needed. Overall, I compiled the existing riverine POC and DOC radiocarbon data and associated parameters and demonstrated that latitude and the ^{13}C of both OC size fractions were primary driving factors determining riverine DOC age when both POC and DOC radiocarbon were

examined (Figure 16). Furthermore, I was able to establish significant relationships between elevation, land use, and vegetation with the age of organic carbon found in rivers. The multivariate linear regression outputs of my study provide a conceptual theory that allows for new insight into our understanding of the biogeochemical interactions of both DOC and POC on a global scale. By integrating current knowledge on how riverine organic carbon age is impacted by latitude, discharge, elevation, slope, vegetation and land cover, we gain a better understanding of how the carbon cycle in aquatic systems will be altered by future climate change and land use change.

V. LITERATURE CITED

Alin, S. R., Aalto, R., Goni, M. A., Richey, J. E., and Dietrich, W. E. (2008). Biogeochemical characterization of carbon sources in the Strickland and Fly rivers, Papua New Guinea. *Journal of Geophysical Research-Earth Surface, 113*(F1).

Amon, R. M. W., Rinehart, A. J., Duan, S., Louchouarn, P., Prokushkin, A., and Guggenberger, G. (2012). Dissolved organic matter sources in large Arctic rivers. *Geochimica Et Cosmochimica Acta, 94*, 217-237.

Aramaki, T., Nagao, S., Nakamura, Y., Uchida, M., and Shibata, Y. (2010). The effects of rainfall on carbon isotopes of POC in the Teshio River, Northern Japan. *Radiocarbon, 52*(2), 808-814.

Aufdenkampe, A. K., Mayorga, E., Raymond, P. A., Melack, J. M., Doney, S. C., and Alin, S. R. (2011). Riverine coupling of biogeochemical cycles between land, oceans, and atmosphere. *Frontiers in Ecology and the Environment, 9*(1), 53-60.

Barros, N., Cole, J. J., Tranvik, L. J., Prairie, Y. T., Bastviken, D., Huszar, V. L. M., et al. (2011). Carbon emission from hydroelectric reservoirs linked to reservoir age and latitude. *Nature Geoscience, 4*(9), 593-596.

Bauer, J.E. and Bianchi, T.S. (2011). Dissolved organic carbon cycling and transformation. In:Wolanski E and McLusky DS (eds.) *Treatise on Estuarine and Coastal Science*. Waltham: Academic Press. 5, 7-67.

Benner, R., Benitez-Nelson, B., Kaiser, K., and Amon, R. M. W. (2004). Export of young terrigenous dissolved organic carbon from rivers to the Arctic Ocean. *Geophysical Research Letters, 31*(5).

Bianchi T.S. and Bauer J.E. (2011). Particulate organic carbon cycling and transformation. In: Wolanski E and McLusky DS (eds.) *Treatise on Estuarine and Coastal Science*. Waltham: Academic Press. 5, 69-117.

Bonan, G.B., Levis, S., Sitch, S., Vertenstein, M., and Oleson, K.W. (2003). A dynamic global vegetation model for use with climate models: concepts and description of simulated vegetation dynamics. *Global Change Biology.* 9, 1543-1566.

Burns, K. A., Hernes, P. J., Brinkman, D., Poulsen, A., and Benner, R. (2008). Dispersion and cycling of organic matter from the Sepik River outflow to the Papua New Guinea coast as determined from biomarkers. *Organic Geochemistry, 39*(12), 1747-1764.

Butman, D., Raymond, P. A., Butler, K., and Aiken, G. (2012). Relationships between delta C-14 and the molecular quality of dissolved organic carbon in rivers draining to the coast from the conterminous United States. *Global Biogeochemical Cycles, 26*.

Caraco, N., Bauer, J. E., Cole, J. J., Petsch, S., and Raymond, P. (2010). Millennial-aged organic carbon subsidies to a modern river food web. *Ecology, 91*(8), 2385-2393.

Cole, J. J., and Caraco, N. F. (2001). Carbon in catchments: connecting terrestrial carbon losses with aquatic metabolism. *Marine and Freshwater Research, 52*(1), 101-110.

Cole, J. J., Prairie, Y. T., Caraco, N. F., McDowell, W. H., Tranvik, L. J., and Striegl, R. G. (2007). Plumbing the global carbon cycle: Integrating inland waters into the terrestrial carbon budget. *Ecosystems, 10*(1), 171-184.

Danielson, J., and Gesch, D. (2008). An enhanced global elevation model generalized from multiple higher resolution source datasets (Vol. 37): The International Archives of the Photogrammetry, Remote Sensing and Spatial Information Sciences.

Davis, J., and Benner, R. (2007). Quantitative estimates of labile and semi-labile dissolved organic carbon in the western Arctic Ocean: A molecular approach. *Limnology and Oceanography, 52*(6), 2434-2444.

Ellis, E. E., Keil, R. G., Ingalls, A. E., Richey, J. E., and Alin, S. R. (2012). Seasonal variability in the sources of particulate organic matter of the Mekong River as discerned by elemental and lignin analyses. *Journal of Geophysical Research-Biogeosciences, 117*.

Evans, C. D., Freeman, C., Cork, L. G., Thomas, D. N., Reynolds, B., and Billett, M. F. (2007). Evidence against recent climate-induced destabilisation of soil carbon from C-14 analysis of riverine dissolved organic matter. *Geophysical Research Letters, 34*(7).

Galy, V., and Eglinton, T. (2011). Protracted storage of biospheric carbon in the Ganges-Brahmaputra basin. *Nature Geoscience, 4*(12), 843-847.

Galy, V., France-Lanord, C., and Lartiges, B. (2008). Loading and fate of particulate organic carbon from the Himalaya to the Ganga-Brahmaputra delta. *Geochimica Et Cosmochimica Acta, 72*(7), 1767-1787.

Goni, M. A., Hatten, J. A., Wheatcroft, R. A., and Borgeld, J. C. (2012). Particulate organic matter export by two contrasting small mountainous rivers from the Pacific Northwest, U.S.A. *Journal of Geophysical Research: Biogeosciences. 118*(1), 112-134.

Gordon, E. S., and Goni, M. A. (2003). Sources and distribution of terrigenous organic matter delivered by the Atchafalaya River to sediments in the northern Gulf of Mexico. *Geochimica Et Cosmochimica Acta, 67*(13), 2359-2375.

Griffith, D. R., Barnes, R. T., and Raymond, P. A. (2009). Inputs of Fossil Carbon from Wastewater Treatment Plants to US Rivers and Oceans. *Environmental Science and Technology, 43*(15), 5647-5651.

Griffith, D. R., and Raymond, P. A. (2011). Multiple-source heterotrophy fueled by aged organic carbon in an urbanized estuary. *Marine Chemistry, 124*(1-4), 14-22.

Gu, C. L., Hu, L. Q., Zhang, X. M., Wang, X. D., and Guo, J. (2011). Climate change and urbanization in the Yangtze River Delta. *Habitat International, 35*(4), 544-552.

Guo, L.D. and Macdonald, R.W. (2006). Source and transport of terrigenous organic matter in the upper Yukon River: Evidence from isotope ($\delta^{13}C$, $\Delta^{14}C$, and $\delta^{15}C$) composition of dissolved, colloidal, and particulate phases. *Global Biogeochemical Cycles, 20*(GB2011).

Guo, L. D., Ping, C. L., and Macdonald, R. W. (2007). Mobilization pathways of organic carbon from permafrost to arctic rivers in a changing climate. *Geophysical Research Letters, 34*(13).

Hatten, J. A., Goni, M. A., and Wheatcroft, R. A. (2012). Chemical characteristics of particulate organic matter from a small, mountainous river system in the Oregon Coast Range, USA. *Biogeochemistry, 107*(1-3), 43-66.

Hedges, J. I., Ertel, J. R., Quay, P. D., Grootes, P. M., Richey, J. E., and Devol, A. H. (1986). Organic C-14 in the Amazon River system. *Science, 231*(4742), 1129-1131.

Helie, J. F., and Hillaire-Marcel, C. (2006). Sources of particulate and dissolved organic carbon in the St Lawrence River: isotopic approach. *Hydrological Processes, 20*(9), 1945-1959.

Hilton, R. G., Galy, A., Hovius, N., Horng, M. J., and Chen, H. E. (2010). The isotopic composition of particulate organic carbon in mountain rivers of Taiwan. *Geochimica Et Cosmochimica Acta, 74*(11), 3164-3181.

Hobbie, S. E., Schimel, J. P., Trumbore, S. E., and Randerson, J. R. (2000). Controls over carbon storage and turnover in high-latitude soils. *Global Change Biology, 6*, 196-210.

Hossler, K., and Bauer, J. E. (2012). Estimation of riverine carbon and organic matter source contributions using time-based isotope mixing models. *Journal of Geophysical Research-Biogeosciences, 117*.

Kao, S. J., and Liu, K. K. (1996). Particulate organic carbon export from a subtropical mountainous river (Lanyang Hsi) in Taiwan. *Limnology and Oceanography, 41*(8), 1749-1757.

Komada, T., Druffel, E. R. M., and Trumbore, S. E. (2004). Oceanic export of relict carbon by small mountainous rivers. *Geophysical Research Letters, 31*(7).

Lapierre, J. F., and del Giorgio, P. A. (2012). Geographical and environmental drivers of regional differences in the lake pCO(2) versus DOC relationship across northern landscapes. *Journal of Geophysical Research-Biogeosciences, 117*.

Leithold, E. L., Blair, N. E., and Perkey, D. W. (2006). Geomorphologic controls on the age of particulate organic carbon from small mountainous and upland rivers. *Global Biogeochemical Cycles, 20*(3).

Longworth, B. E., Petsch, S. T., Raymond, P. A., and Bauer, J. E. (2007). Linking lithology and land use to sources of dissolved and particulate organic matter in headwaters of a temperate, passive-margin river system. *Geochimica Et Cosmochimica Acta, 71*(17), 4233-4250.

Masiello, C. A., and Druffel, E. R. M. (2001). Carbon isotope geochemistry of the Santa Clara River. *Global Biogeochemical Cycles, 15*(2), 407-416.

Mayorga, E., Aufdenkampe, A. K., Masiello, C. A., Krusche, A. V., Hedges, J. I., and Quay, P. D. (2005). Young organic matter as a source of carbon dioxide outgassing from Amazonian rivers. *Nature, 436*(7050), 538-541.

McCallister, S. L., Bauer, J. E., Cherrier, J. E., and Ducklow, H. W. (2004). Assessing sources and ages of organic matter supporting river and estuarine bacterial production: A multiple-isotope (Delta C-14, delta C-13, and delta N-15) approach. *Limnology and Oceanography, 49*(5), 1687-1702.

McCallister, S. L., Bauer, J. E., Ducklow, H. W., and Canuel, E. A. (2006). Sources of estuarine dissolved and particulate organic matter: A multi-tracer approach. *Organic Geochemistry, 37*(4), 454-468.

McCallister, S. L., and del Giorgio, P. A. (2008). Direct measurement of the delta C-13 signature of carbon respired by bacteria in lakes: Linkages to potential carbon sources, ecosystem baseline metabolism, and CO2 fluxes. *Limnology and Oceanography, 53*(4), 1204-1216.

McCallister, S. L., and del Giorgio, P. A. (2012). Evidence for the respiration of ancient terrestrial organic C in northern temperate lakes and streams. *Proceedings of the National Academy of Sciences of the United States of America, 109*(42), 16963-16968.

McNichol, A., and Aluwihare, L.I. (2007). The power of radiocarbon in biogeochemical studies of the marine carbon cycle: Insights from studies of dissolved and particulate organic carbon (DOC and POC). Luther III, G.W. and Boyle, E.A. Chemical Reviews *107,* 443-466.

Megens, L., van der Plicht, J., and de Leeuw, J. W. (2001). Temporal variations in C-13 and C-14 concentrations in particulate organic matter from the southern North Sea. *Geochimica Et Cosmochimica Acta, 65*(17), 2899-2911.

Meybeck, M. (1982). Carbon, nitrogen, and phosphorus transport by world rivers. *American Journal of Science, 282*(4), 401-450.

Moreira-Turcq, P., Bonnet, M.-P., Amorim, M., Bernardes, M., Lagane, C., and Maurice, L. (2013). Seasonal variability in concentration, composition, age and fluxes of particulate organic carbon exchanged between the floodplain and Amazon River. *Global Biogeochemical Cycles.* doi: 10.1002/gbc.20022.

Moyer, R., Bauer, J., and Grottoli, A. (2012). Carbon isotope biogeochemistry of tropical small mountainous river, estuarine, and coastal systems of Puerto Rico. *Biogeochemistry*. doi: 10.1007/s10533-012-9751-y.

Nagao, S., Aramaki, T., Seki, O., Uchida, M., and Shibata, Y. (2010). Carbon isotopes and lignin composition of POC in a small river in Bekanbeushi Moor, northern Japan. *Nuclear Instruments and Methods in Physics Research Section B-Beam Interactions with Materials and Atoms, 268*(7-8), 1098-1101.

Neff, J. C., Finlay, J. C., Zimov, S. A., Davydov, S. P., Carrasco, J. J., and Schuur, E. A. G. (2006). Seasonal changes in the age and structure of dissolved organic carbon in Siberian rivers and streams. *Geophysical Research Letters, 33*(23).

Raymond, P. A., and Bauer, J. E. (2001a). Riverine export of aged terrestrial organic matter to the North Atlantic Ocean. *Nature, 409*(6819), 497-500.

Raymond, P. A., and Bauer, J. E. (2001b). Use of (14)C and (13)C natural abundances for evaluating riverine, estuarine, and coastal DOC and POC sources and cycling: a review and synthesis. *Organic Geochemistry, 32*(4), 469-485.

Raymond, P. A., Bauer, J. E., Caraco, N. F., Cole, J. J., Longworth, B., and Petsch, S. T. (2004). Controls on the variability of organic matter and dissolved inorganic carbon ages in northeast US rivers. *Marine Chemistry, 92*(1-4), 353-366.

Raymond, P. A., and Hopkinson, C. S. (2003). Ecosystem modulation of dissolved carbon age in a temperate marsh-dominated estuary. *Ecosystems, 6*(7), 694-705.

Raymond, P. A., McClelland, J. W., Holmes, R. M., Zhulidov, A. V., Mull, K., and Peterson, B. J. (2007). Flux and age of dissolved organic carbon exported to the Arctic Ocean: A carbon isotopic study of the five largest arctic rivers. *Global Biogeochemical Cycles, 21*(4).

Rosenheim, B. E., and Galy, V. (2012). Direct measurement of riverine particulate organic carbon age structure. *Geophysical Research Letters, 39*.

Rosenheim, B. E., Roe, K. M., and Roberts, B. J. (2013). River discharge influences on particulat organic carbon age structure in the Mississippi/Atchafalaya river system. *Global Biogechemical Cycles.* 27(1) 154-166..

Running, S. W., Loveland, T. R., Pierce, L. L., Nemani, R., and Hunt, E. R. (1995). A remote-sensing based vegetation classification for global land-cover analysis.*Remote Sensing of Environment, 51*(1), 39-48.

Sickman, J. O., DiGiorgio, C. L., Davisson, M. L., Lucero, D. M., and Bergamaschi, B. (2010). Identifying sources of dissolved organic carbon in agriculturally dominated rivers using radiocarbon age dating: Sacramento-San Joaquin River Basin, California. *Biogeochemistry, 99*(1-3), 79-96.

Spencer, R. G. M., Hernes, P. J., Aufdenkampe, A. K., Baker, A., Gulliver, P., and Stubbins, A. (2012). An initial investigation into the organic matter biogeochemistry of the Congo River. *Geochimica Et Cosmochimica Acta, 84*, 614-627.

Spiker, E. C., and Rubin, M. (1975). Petroleum pollutants in surface and groundwater as indicated by C-14 activity of dissolved organic carbon. *Science, 187*(4171), 61-64.

Townsend-Small, A., Noguera, J. L., McClain, M. E., and Brandes, J. A. (2007). Radiocarbon and stable isotope geochemistry of organic matter in the Amazon headwaters, Peruvian Andes. *Global Biogeochemical Cycles, 21*(2).

Tranvik, L. J., Downing, J. A., Cotner, J. B., Loiselle, S. A., Striegl, R. G., and Ballatore, T. J. (2009). Lakes and reservoirs as regulators of carbon cycling and climate. *Limnology and Oceanography, 54*(6), 2298-2314.

Trumbore, S. (2000). Age of soil organic matter and soil respiration: Radiocarbon constraints on belowground C dynamics. *Ecological Applications, 10*(2), 399-411.

Trumbore, S.E. and Druffel, E.R.M. (1995). Carbon Isotopes on Characterizing Sources and Turnover of Nonliving Organic Matter. *The Role of Nonliving Organic Matter in the Earth's Carbon Cycle.* Ed. Dahlem Editorial Staff. England, 1995. 8-22. Print.

Wang, S. J., Yan, M., Yan, Y. X., Shi, C. X., and He, L. (2012). Contributions of climate change and human activities to the changes in runoff increment in different sections of the Yellow River. *Quaternary International, 282*, 66-77.

Wei, X. G., Yi, W. X., Shen, C. D., Yechieli, Y., Li, N. L., and Ding, P. (2010). C-14 as a tool for evaluating riverine POC sources and erosion of the Zhujiang (Pearl River) drainage basin, South China. *Nuclear Instruments and Methods in Physics Research Section B-Beam Interactions with Materials and Atoms, 268*(7-8), 1094-1097.

VI. LIST OF DATABASES

FAO/IISA. (2000). Global Agro-Ecological Zones (GAEZ) CD-ROM. Retrieved from Global Change Master Directory NASA. < http://gcmd.nasa.gov/records/GCMD_FAO_GAEZ .html>. Accessed 5/7/2014.

Global Runoff Data Centre (2007): Major River Basins of the World / Global Runoff Data Centre. Koblenz, Germany: Federal Institute of Hydrology (BfG). < http://blogs.esri.com/esri/arcgis /2011/ 08/05/global-hydro-data-its-here-here-here/>. Accessed 5/7/2014.

Goddard Institute for Space Studies/Earth Sciences Directorate/Goddard Space Flight Center/NASA. 1983. Matthew's GISS Global 1-Degree Vegetation, Land-use and Albedo Data. Research Data Archive at the National Center for Atmospheric Research, Computational and Information Systems Laboratory. http://rda.ucar.edu/datasets/ds765.0. Accessed 03/15/2013.

GTOPO30. United States Geological Survey. Department of the Interior. /https://lta.cr.usgs. gov/GTOPO30. Accessed 5/7/14.

PARTNERS. (2012). Great Arctic Rivers Observatory. < http://www.arcticgreatrivers.org/data. html>. Accessed 5/7/14.

VII. APPENDIX A—TABLES

Table 1: Dominant land cover categories and vegetation grouping based on classification of original datasets. Abbreviations for each group are also provided. Numbers in the table correspond to the differing classifications outlined by the legends from Figure 2A and 2B, respectively.

Land Cover Group	Mixed	M	10
	Built Up	BU	9
	Grass and Woodland	GW	3, 7
	Forested	F	2, 6
	Cultivated	C	1, 5
	Barren	B	11
Vegetation Group	Tundra	T	(Arctic/alpine tundra, and mossy bog) 22
	Evergreen Needleleaf	EN	(Needleleaved evergreen tropical and temperate forest, woodland, and shrubland) 4, 7, 8, 14, 17, 18
	Deciduous Mixed	DM	(Deciduous forest, woodland, and shrubland) 9, 10, 11, 15, 16, 19, 20, 21
	Evergreen Broadleaf	EB	(Broadleaved evergreen tropical/subtropical and temperate rainforest, forest, and woodland) 1, 2, 3, 5, 6, 12, 13
	Grasses	G	(Grassland (tall/short), shrub cover, no shrub, no woody cover, and forb formations) 23, 24, 25, 26, 27, 28, 29

Table 2: Published values of organic carbon in global rivers (ranges reported when available)

	DOC			POC			
River System	**Concentration (µM)**	**$\delta^{13}C$ range (‰)**	**$\Delta^{14}C$ range (‰)**	**Concentration (µM)**	**$\delta^{13}C$ range (‰)**	**$\Delta^{14}C$ range (‰)**	**Authors**
Alsea				49.2 to 2017	-26.4 to -25.6	-8 to 32	Hatten et al. (2012)
Altamaha	833.3	-26.8	73				Butman et al. (2012)
Amazon	14.2 to 853.3	-29.9 to -21.8	-222 to 336	49.3 to 589.2	-30.7 to -23.7	-382 to 142	Hedges et al. (1986); Mayorga et al. (2005); Moreira-Turcq et al. (2013); Raymond et al. (2001b); Townsend-Small et al. (2012)
Atchafalaya					-25.0 to -23.8	-287 to -51	Rosenheim and Galy (2012)
Bekanbeushi				105.8 to 400.8	-29.1 to -28.7	-103 to 20	Nagao et al. (2010)
Boluo				66.67 to 108.3	-23.8 to -22.0	-193 to -65	Wei et al. (2010)
Brahmaputra						-474 to -348	Galy et al. (2007); Galy and Eglinton (2011)
Colorado	241.7	-25.7	-93				Butman et al. (2012)
Columbia	166.7	-25.21	18				Butman et al. (2012)
Congo				107.5 to 148.3	-28.5 to -23.9	-60 to -27	Spencer et al. (2012)
Connecticut	283.3	-27.6 to -26.7	-55 to 60		-29.5 to -25.5	-175 to -60	Butman et al. (2012); Hossler and Bauer (2012)
Conwy	241.7 to 858.3		22 to 83				Evans et al. (2007)
Delaware	242	-27.5 to -18	-140 to 30	44	-27.5 to -22	-240 to 6	Hossler and Bauer (2012); Raymond et al. (2004)
Eel					-25.7 to -25.4	-532 to -403	Goni et al (2013); Leithold et al. (2006)
Ganges						-311 to -247	Galy and Eglinton (2011)

Table 2 (cont)

River System	DOC Concentration (µM)	DOC $\delta^{13}C$ range (‰)	DOC $\Delta^{14}C$ range (‰)	POC Concentration (µM)	POC $\delta^{13}C$ range (‰)	POC $\Delta^{14}C$ range (‰)	Authors
Hudson	183.0 to 898.0	-29.7 to -25.0	-158 to 101	14.0 to 1642.0	-29.5 to -23.4	-452 to -20	Butman et al. (2012); Caraco et al. (2010); Cole and Caraco (2001); Griffith et al. (2009); Griffith and Raymond (2011); Hossler and Bauer (2012); Longworth et al. (2007); Raymond et al. (2001b); Raymond et al. (2004);
Ikpikpuk			6				Benner et al. (2004)
James		-28	42				Spiker and Rubin (1975)
Kokolik			-6				Benner et al. (2004)
Kolyma	240.0 to 855.0	-32.2 to -24.2	-87 to 116	6.6 to 121.3	-35.1 to -26.5		Neff et al. (2006); PARTNERS
Kosi						-293 to -191	Galy and Eglinton (2011)
Lajas	337.0 to 712.0	-26.9 to -25.3	-258 to 16	711.0	-28.7 to -25.7	-68 to -13	Moyer et al. (2012)
Lanyang His				95.0 to 145.8		-875 to -716	Kao and Liu (1996)
Lena	433.0 to 1233.0	-28.3 to 25.2	-39 to 121	6.6 to 343.6	-36 to -25.2		PARTNERS
LiWu				850 to 20200		-956 to -24	Hilton et al. (2010)
MacKenzie	259.0 to 461.8	-27.3 to -20.5	-169 to 37	5.9 to 285.8	-33.7 to -22.1	-625 to -530	Guo et al. (2007); PARTNERS
Makou				102.5 to 245.8	-26.1 to -22.9	-425 to -132	Wei et al. (2010)
Meuse				366.7	-27.1	-40	Megens et al. (2001)
Mississippi					-27.1 to -22.4	-317 to -15	Rosenheim and Galy (2012)
Mobile	497.7	-20.2	24				Butman et al. (2012)
Mt. Britton	67.0	-25.8	43	254.0	-21	21	Moyer et al. (2012)
Narayani						-616 to -515	Galy and Eglinton (2011)
Ob'	458.3 to 913.7	-29.1 to -25.0	-114 to 307	61.9 to 189.7	-35.4 to -29.7		Benner et al. (2004), PARTNERS

Table 2 (Cont)

River System	DOC			POC			Authors
	Concentration (µM)	$\delta^{13}C$ range (‰)	$\Delta^{14}C$ range (‰)	Concentration (µM)	$\delta^{13}C$ range (‰)	$\Delta^{14}C$ range (‰)	
Parker	503.0 to 1001.0	-30.3 to -28.4	-4 to 111	18.0 to 208.0	-33.7 to -30.0	-190 to 47	Raymond and Bauer (2001b); Raymond and Hopkinson (2003)
Potomac	275.0	-32.4 to -25.9	-41 to 365		-31.0 to -24.0	-125 to -40	Butman et al. (2012); Hossler and Bauer (2012); Spiker and Rubin (1975)
Rappahannock		-31.9	-91				Spiker and Rubin (1975)
Rhine				258.3 to 491.7	-29.7 to -27.0	-107 to -79	Megens et al. (2001)
Rio Fajardo	57.0 to 202.0	-29.3 to -19.3	-62.0 to 13	19.0 to 289.0	-26.8 to -17.0	-36 to 17	Moyer et al. (2012)
Rio Loco	113.0 to 444.0	-32 to -23.4	-208 to 33	169.0 to 3328.0	-37.9 to -24.7	-92 to -13	Moyer et al. (2012)
Sepik	197.5	-27.4		733.3	-26.5		Burns et al. (2008)
Yangtze River	151.0 to 228.0	-32.2 to -28.8	-183 to -44		-25.5 to -23.1	-129 to -103	Wang et al. (2012)
Rio Grande	400.0	-27.2	-63				Butman et al. (2012)
Roanoke		-28.4 to -27.8	-60 to 90		-30.5 to 27.0	-80 to -10	Hossler and Bauer (2012)
Sacramento	42.5 to 216.7	-26.5 to -21.6	-152 to 383				Butman et al. (2012); Sickman et al. (2010)
Sagavanirktok	63.0 to 118.0	-27.8 to -27.2	-463 to -242	52.0 to 158.0	-27.0 to -26.9	-466 to -465	Guo et al. (2007)
San Joaquin	40.0 to 316.7	-25.8 to -25.2	-218 to 4				Butman et al. (2012); Sickman et al. (2010)
Santa Clara	319.0 to 944.0	-27.8 to -25.0	-186 to -62	6660.0 to 18110.0	-27.1 to -19.7	-657 to -139	Komada et al. (2004); Masiello and Druffel (2001)
Siuslaw					-27.1 to -26.8	7 to 39	Leithold et al. (2006)
St. Lawrence	225.0 to 320.8	-26.4 to -25.4	21.8 to 35				Butman et al. (2012); Hélie and Hillaire-Marcel (2006)
Susquehanna	113.0 to 225.0	-27.5 to -19.5	-236 to 5	20.0	-34.0 to -25.0	-220 to -61	Butman et al. (2012); Hossler and Bauer (2012); Raymond et al. (2004); Spiker and Rubin (1975)

Table 2 (Cont)

River System	DOC			POC			
River System	**Concentration (µM)**	**$\delta^{13}C$ range (‰)**	**$\Delta^{14}C$ range (‰)**	**Concentration (µM)**	**$\delta^{13}C$ range (‰)**	**$\Delta^{14}C$ range (‰)**	**Authors**
Teshio				11.4 to 252.5	-26.6 to -25.3	-56 to -10	Aramaki et al. (2010)
Tokachi					-26.3 to -25.0	-242 to -101	Nagao et al. (2010)
Umpqua					-26.4 to -24.0	-48 to -41	Goni et al. (2013)
Waiapu					-25.6 to -25.2	-765 to -698	Leithold et al. (2006)
Waipaoa					-26.7 to -26.1	-599 to -263	Leithold et al. (2006)
Yellow	174.0 to 231.0	-32.1 to -25.6	-131 to -55		-25.6 to -23.4	-635 to -405	Wang et al. (2012)
Yenisey	241.7 to 1079.0	-27.6 to -20.4	-12 to 150	6.2 to 75.9	-33.4 to -27.6		Benner et al. (2004); PARTNERS
York	390.0 to 713.0	-28.8 to -27.9	159 to 257	30.0			Raymond and Bauer (2001a); Raymond and Bauer (2001b); Raymond et al. (2004)
Yukon	218.0 to 1258.0	-28.8 to -24.2	-162 to 91	23.0 to 642.0	-36.6 to -24.9	-558 to -253	Guo and Macdonald (2006); Guo et al. (2007); PARTNERS
Zengjiang				258.0 to 1134.0	-26.6 to -23.9	-165 to -33	Gao et al. (2007)

Table 3: Mean values of $\delta^{13}C$ and $\Delta^{14}C$ of DOC, POC for the classes within land cover, vegetation, and climate categories. Results for a one-way ANOVA comparing the difference in means for $DO^{14}C$ (‰) and $PO^{14}C$ (‰) are also shown. Mean values with similar letters in superscript have means that are not significantly different from each other at α=0.05.

		$DO^{13}C$ (‰)	$PO^{13}C$ (‰)	$DO^{14}C$ (‰)			$PO^{14}C$ (‰)		
		Mean	Mean	Mean	F Statistic	Approximate Age	Mean	F Statistic	Approximate Age
Land Cover Group	Mixed	-27.1 ± 1.9	-28.4 ± 3.5	-3 ± 89^{b}		Modern	-169 ± 168^{ab}		1450
	Built Up	-27.3 ± 1.9	-27.2 ± 2.3	20 ± 132^{ab}		Modern	-72 ± 31^{a}		540
	Grass and Woodland	-25.7 ± 2.1	-27.2 ± 3.1	5 ± 115^{b}	8.565 (5,248) p <0.001	Modern	-266 ± 228^{b}	4.239 (4.288) p=0.002	2450
	Forested	-27.4 ± 1.9	-26.9 ± 2.5	59 ± 110^{bc}		Modern	-187 ± 210^{ab}		1600
	Cultivated	-27.8 ± 3.0	-25.2 ± 1.9	-60 ± 139^{a}		440	-351 ± 283^{b}		3400
	Barren	-29.2 ± 0.1		216 ± 107^{c}		Modern			
Vegetation Group	Tundra	-26.9 ± 1.3	-28.5 ± 2.6	-52 ± 130^{bc}		360	-424 ± 92^{c}		4350
	Evergreen Needleleaf	-25.9 ± 2.0	-26.9 ± 2.5	-13 ± 106^{bc}		50	-158 ± 206^{a}		1300
	Deciduous Mixed	-27.0 ± 2.0	-28.2 ± 3.1	19 ± 89^{ab}	9.564 (5,248) p<0.001	Modern	-167 ± 132^{ab}	6.377 (4,288) p<0.001	1400
	Evergreen Broadleaf	-27.7 ± 2.3	-25.7 ± 2.9	113 ± 137^{a}		Modern	-225 ± 268^{ab}		2000
	Grasses	-24.9 ± 2.1	-25.9 ± 1.2	-33 ± 183^{c}		210	-305 ± 269^{bc}		2900
	Climate Group	Boreal/Arctic		16 ± 89	16.748 (2,250) p<0.001	Modern	-375 ± 181	5.935 (2,290) p=0.003	3650
		Temperate		-6 ± 106		Modern	-224 ± 229		2000
		Tropical		110 ± 143		Modern	-115 ±121		900

Table 4: Descriptive statistics of the riverine organic carbon observations.

	# of Observations	Range	Min	Max	Mean	Std Dev
DOC (μM)	229	2810.8	14.2	2825.0	459.2	329.2
$DO^{13}C$ (‰)	273	14.4	-32.4	-18.0	-27.0	2.1
$DO^{14}C$ (‰)	275	846	-463	383	22	114
POC (μM)	234	20194.1	5.911	20200.0	687.7	2520.0
$PO^{13}C$ (‰)	252	21.0	-38	-17.0	-27.4	3.0
$PO^{14}C$ (‰)	297	1099	-957	142	-204	213

Table 5: Linear relationships between the natural log of DOC Age and natural log of POC Age and environmental factors examined.*indicates the relationships is significant at a level of α=0.05.

	Dependent Variable									
	DOC Age							POC Age		
	Independent Variable									
	DOC (μM)	$DO^{13}C$ (‰)	POC (μM)	$PO^{13}C$ (‰)	POC Age	Latitude	Elevation (m)	POC (μM)	$PO^{13}C$ (‰)	Latitude
n	174	258	131	193	107	253	254	100	239	293
mean	7.81* (Modern)	7.83* (Modern)	7.82* (Modern)	7.85* (Modern)	7.93* (130 yrs)	7.82* (Modern)	7.82* (Modern)	7.78 (1300 yrs)	7.77* (1300 yrs)	7.85 (1450 yrs)
std. dev.	0.3	0.28	0.28	0.26	0.29	0.017	0.28	0.67	0.6	0.7
R^2	0.087	0.079	0.079	0.076	0.256	0.017	0.155	0.032	0.048	0.006
F-statistic	16.333	20.519	11.069	15.631	36.1	4.222	6.219	3.221	11.86	1.831
p value	<0.001	<0.001	0.001	<0.001	<0.001	0.041	0.013	0.076	0.001	0.177
Slope	-3.37E10	0.036	-3.16E10	0.024	0.250	0.002	1.09E4	5.9E5	0.056	-0.003
Intercept	7.965	8.807	7.826	8.521	5.983	7.746	7.807	7.760	9.251	7.930

Table 6: Variables included in the stepwise regressions for the natural log of $DO^{14}C$ age (MLR DO14C), $PO^{14}C$ age (MLR $PO^{14}C$), and $DO^{14}C$ age w/all factors (MLR $DO^{14}C/PO^{14}C$). ns = not statistically significant, * = significant at $\alpha=0.05$

	Variables	B coefficient
MLR DO14C	DOC (μM)	-0.000453^{*}
	$DO^{13}C$ (‰)	0.017^{ns}
	Avg Elevation	0.000126^{*}
	Latitude	0.005^{*}
MLR $PO^{14}C$	POC (μM)	0.000047^{*}
	$PO^{13}C$ (‰)	0.040^{ns}
	Latitude	0.005^{*}
MLR $DO^{14}C/PO^{14}C$	$DO^{13}C$ (‰)	0.072^{*}
	$PO^{13}C$ (‰)	0.049^{*}
	Latitude	0.009^{*}

Table 7: Summary statistics for the best stepwise regression analysis for each of the dependent variables analyzed following the linear regressions in Table 6. Mean in parenthesis is transformed age. The highest Adj. R2 is indicated in bold. * indicates significance at the 0.05 level.

	MLR $DO^{14}C$	MLR $PO^{14}C$	MLR $DO^{14}C/PO^{14}C$
Dependent Variable	$DO^{14}C$ age	$PO^{14}C$ age	$DO^{14}C$ age
		Regression	
n	176	112	43
mean	15 ‰ (7.81)*	-135 ‰ (7.7)*	-12 ‰ (7.9)*
std. dev.	0.302	0.597	0.391
Adj. R^2	0.249	0.158	**0.607**
F-statistic	15.156	7.961	21.853
α	0.05	0.05	0.05
p-value	<0.001	<0.001	<0.001

Table 8: P values for the differences between categorical groups from a post hoc Tukey HSD test. 8A) P-values of differences in Land Cover groups for $DO^{14}C$ and $PO^{14}C$. 8B) P-values of differences in Vegetation groups for $DO^{14}C$ and $PO^{14}C$. 8C) P-values of differences in climate groups for $DO^{14}C$ and $PO^{14}C$. Values in bold indicate the largest differences. * indicates significant differences at a level of $\alpha=0.05$.

8A)	Mixed		Built Up		Grass and Woodland		Forested		Cultivated		Barren	
	$DO^{14}C$	$PO^{14}C$	$DO^{14}C$	$PO^{14}C$	$DO^{14}C$	$PO^{14}C$	$DO^{14}C$	$PO^{14}C$	$DO^{14}C$	$PO^{14}C$	$DO^{14}C$	$PO^{14}C$
Mixed	--	--	1.000	0.581	0.850	0.219	0.003*	0.998	0.025*	**0.038***	**0.013***	--
Built Up	1.000	0.581	--	--	0.994	0.082	0.471	0.456	0.177	**0.014***	**0.027***	--
Grass and Woodland	0.850	0.219	0.994	0.082	--	--	0.255	0.183	0.004*	0.621	**0.033***	--
Forested	0.003*	0.998	0.471	0.456	0.255	0.183	--	--	<0.001*	**0.035***	0.122	--
Cultivated	0.025*	**0.038***	0.177	**0.014***	0.004*	0.621	<0.001*	**0.035***	--	--	**<0.001***	--
Barren	**0.013***	--	**0.027***	--	**0.033***	--	0.122	--	**<0.001***	--	--	--

8B)	Tundra		Evergreen Needleaf		Deciduous Mixed		Evergreen Broadleaf		Grasses	
	$DO^{14}C$	$PO^{14}C$	$DO^{14}C$	$PO^{14}C$	$DO^{14}C$	$PO^{14}C$	$DO^{14}C$	$PO^{14}C$	$DO^{14}C$	$PO^{14}C$
Tundra	--	--	1.000	**<0.001***	0.243	**0.002***	<0.001*	**0.027***	0.684	0.370
Evergreen Needleleaf	1.000	**<0.001***	--	--	0.283	0.633	**<0.001***	0.075	0.593	**0.015***
Deciduous Mixed	0.243	**0.002***	0.283	0.633	--	--	**<0.001***	0.429	0.116	0.930
Evergreen Broadleaf	**<0.001***	**0.027***	**<0.001***	0.075	**<0.001***	0.429	--	--	**0.001***	0.641
Grasses	0.684	0.370	0.593	**0.015***	0.116	0.093	**<0.001***	0.641	--	--

8C)

	Boreal/Arctic		Temperate		Tropical	
	$DO^{14}C$	$PO^{14}C$	$DO^{14}C$	$PO^{14}C$	$DO^{14}C$	$PO^{14}C$
Boreal and Arctic	--	--	0.002*	0.008*	0.005*	**0.002***
Temperate	0.002*	0.008*	--	--	**<0.001***	0.452
Tropical	.005*	**0.002***	**<0.001***	0.452	--	--

VIII. APPENDIX B—FIGURES

1A)

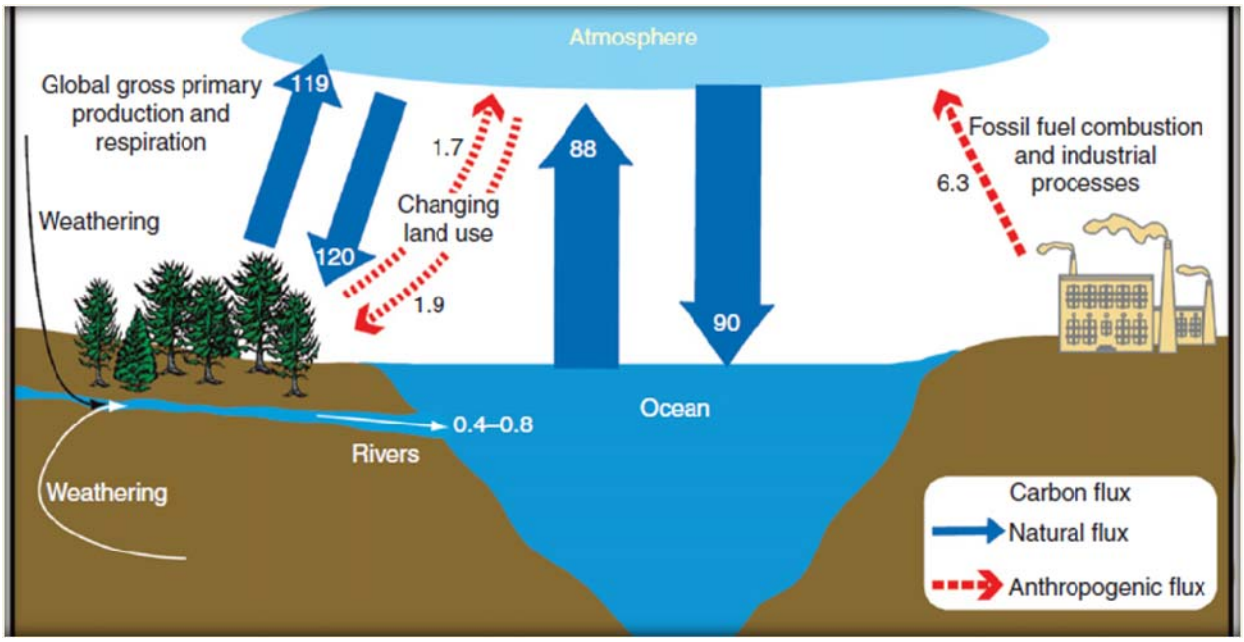

1B)

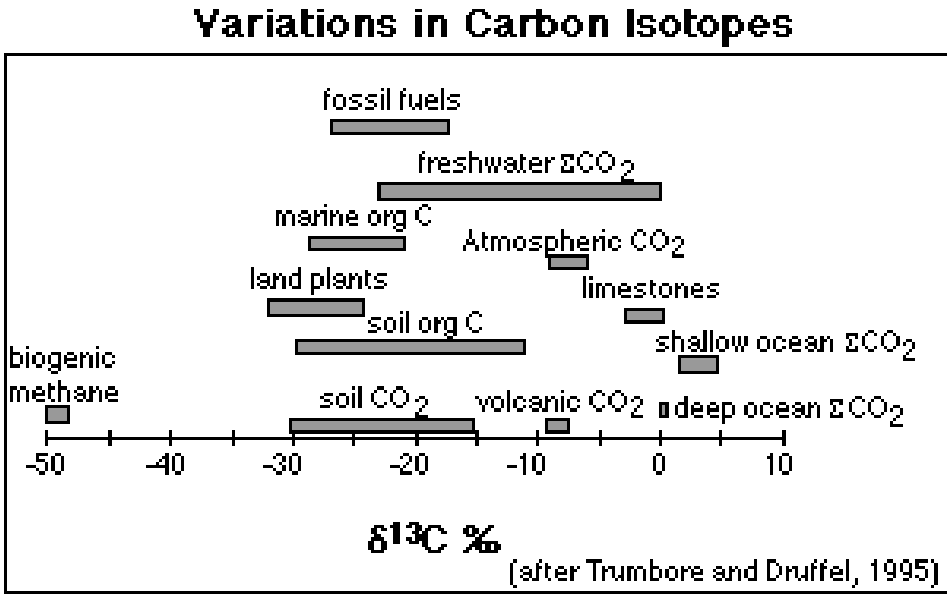

1C)

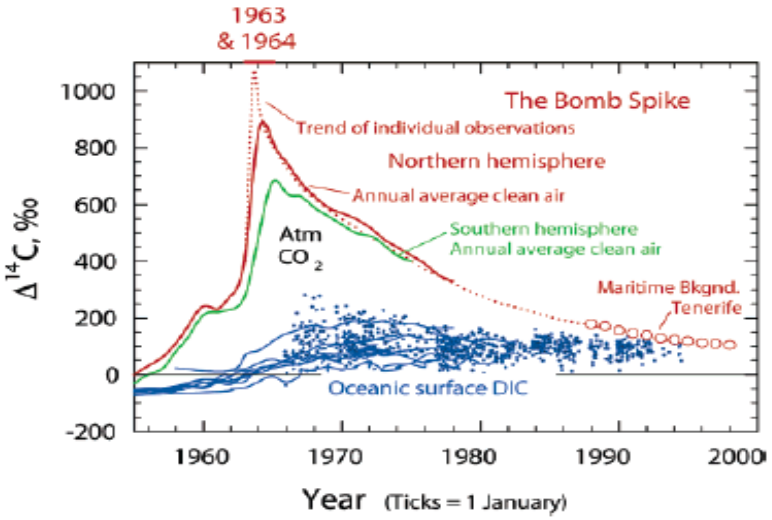

Figure 1: 1A) Global Carbon Cycle fluxes between the three major resevoirs in Gigatons of C yr^{-1} and the impacts of anthropogenic activity from Bauer and Bianchi 2011. 1B) Ranges of variation in $\delta^{13}C$ signatures for different sources of inorganic and organic matter as outlined by Trumbore and Druffel 1995. 1C) Result of nuclear testing on total amount of $\Delta^{14}C$ (‰) found in the atmosphere as seen in McNichol and Aluwihare (2007).

2A)

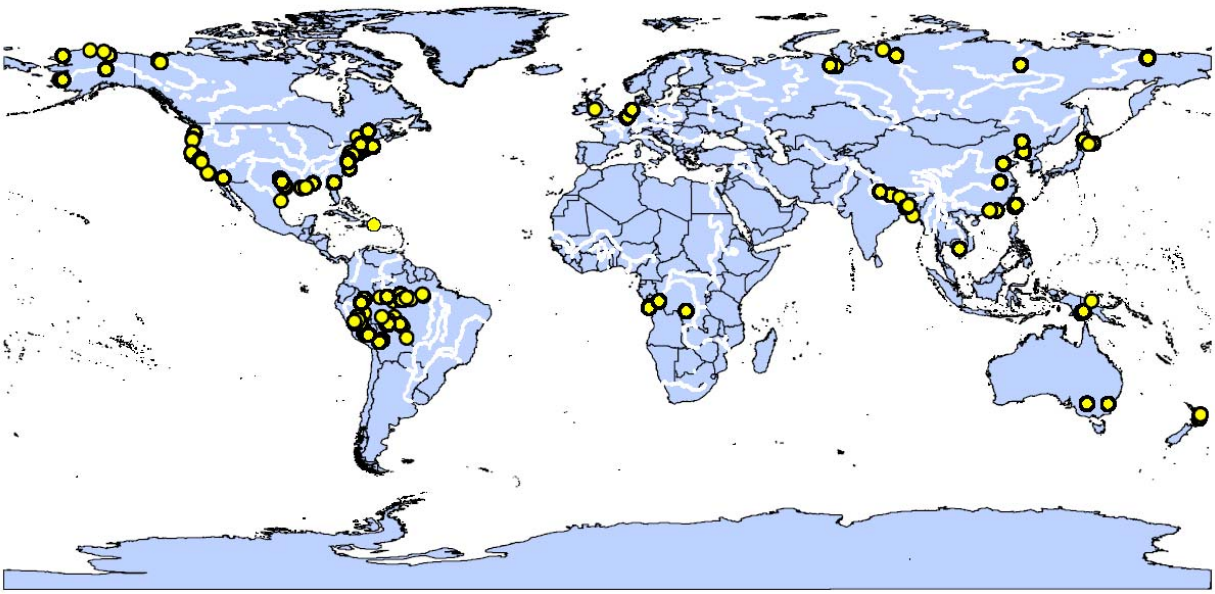

2B)

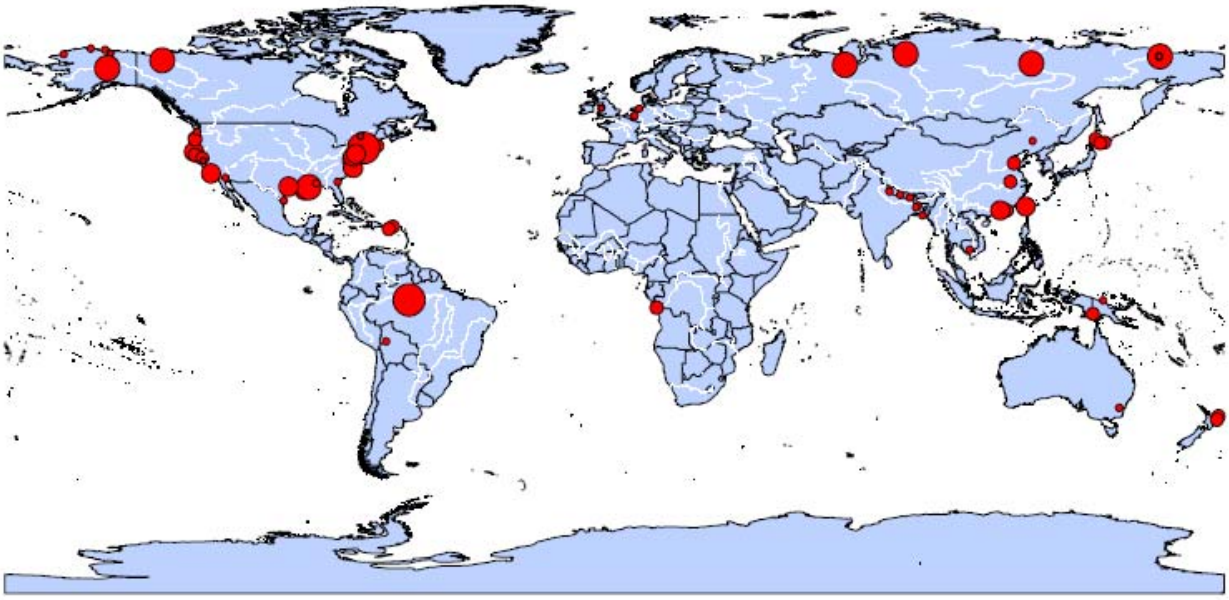

Figure 2: Maps generated by the use of ArcGIS. 2A) Sampling locations of the river systems incorporated into this study. 2B) Frequency of the observations for each river. Larger circles denote heavier sampled rivers relative to least sampled rivers.

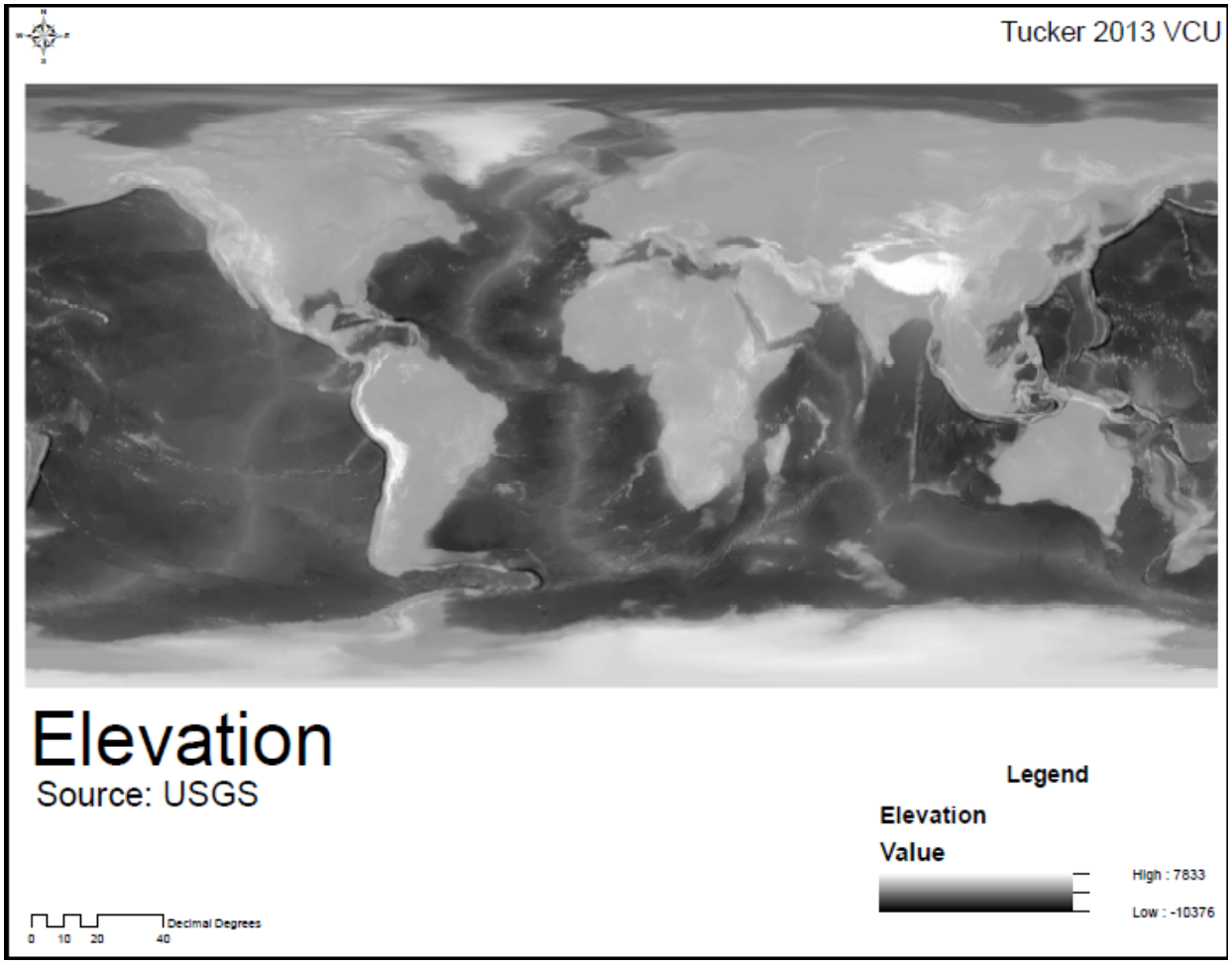

Figure 3: Elevation data provided by USGS and used as a layer in ArcGIS

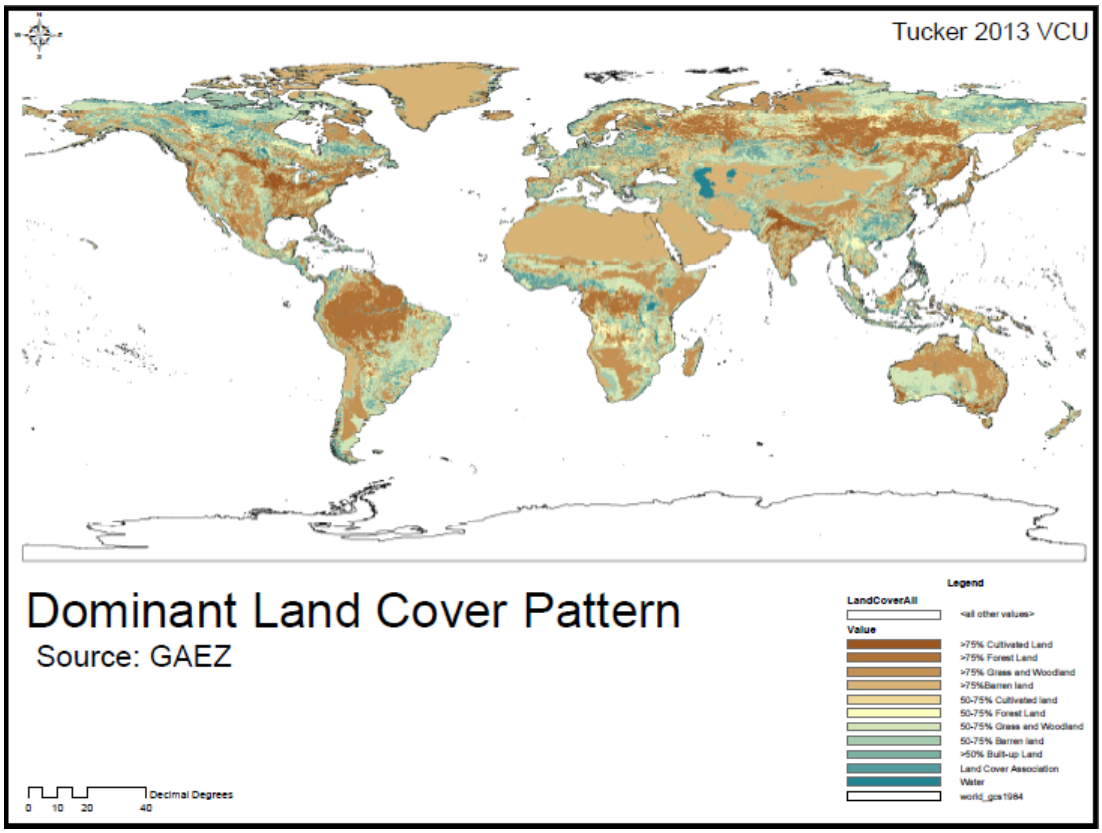

Figure 4: Land cover/use incorporated into this study as obtained from the Food and Agriculture Organization.

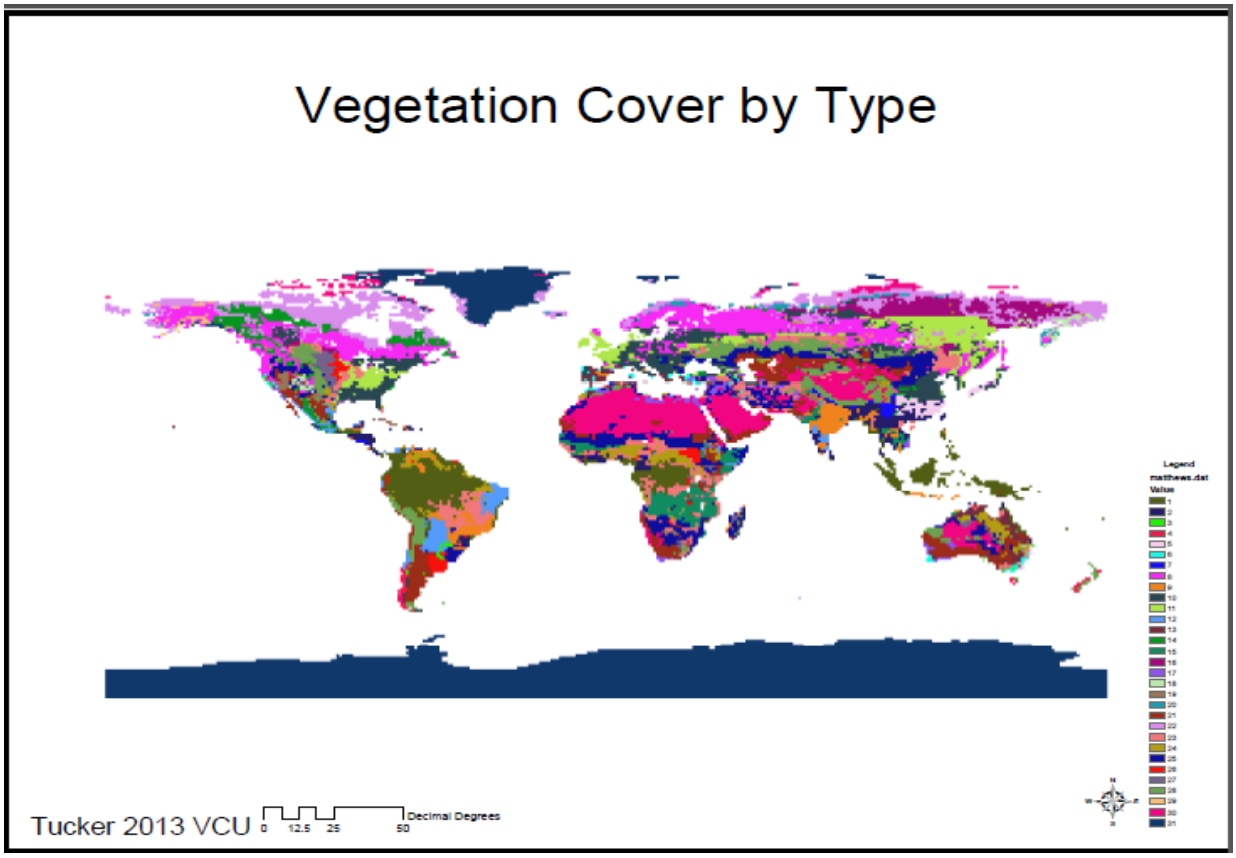

Figure 5: Initial vegetation data incorporated into the study as obtained from the Goddard Institute of Space Studies.

6A)

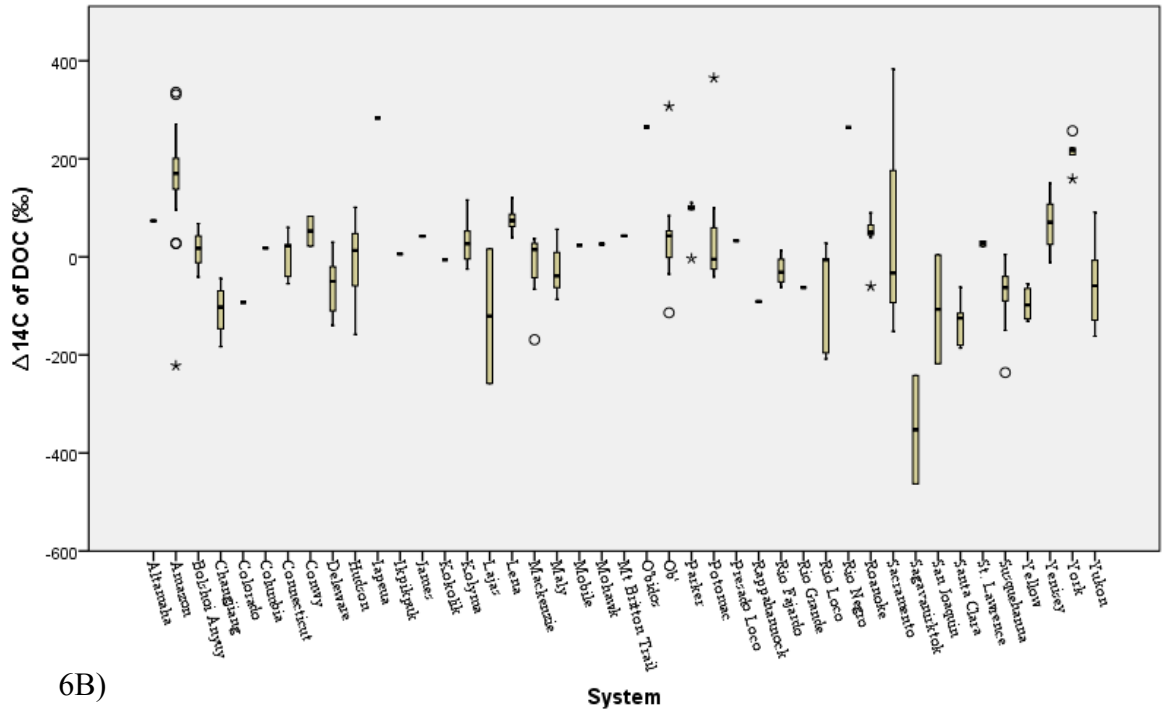

6B)

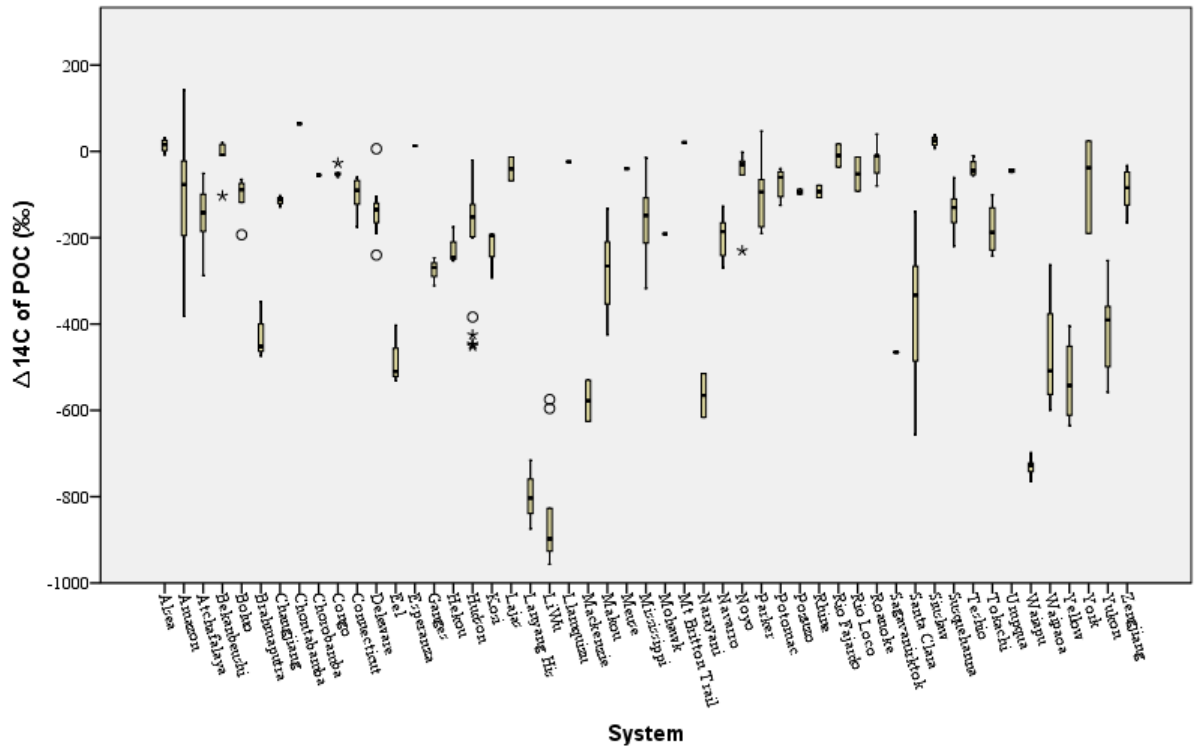

Figure 6: Box and whisker plots outlining the range, mean, and outliers of $\Delta^{14}C$ values included for each river for 6A)$DO^{14}C$ and 6B) $PO^{14}C$. ° indicates outliers. * indicates extreme outliers.

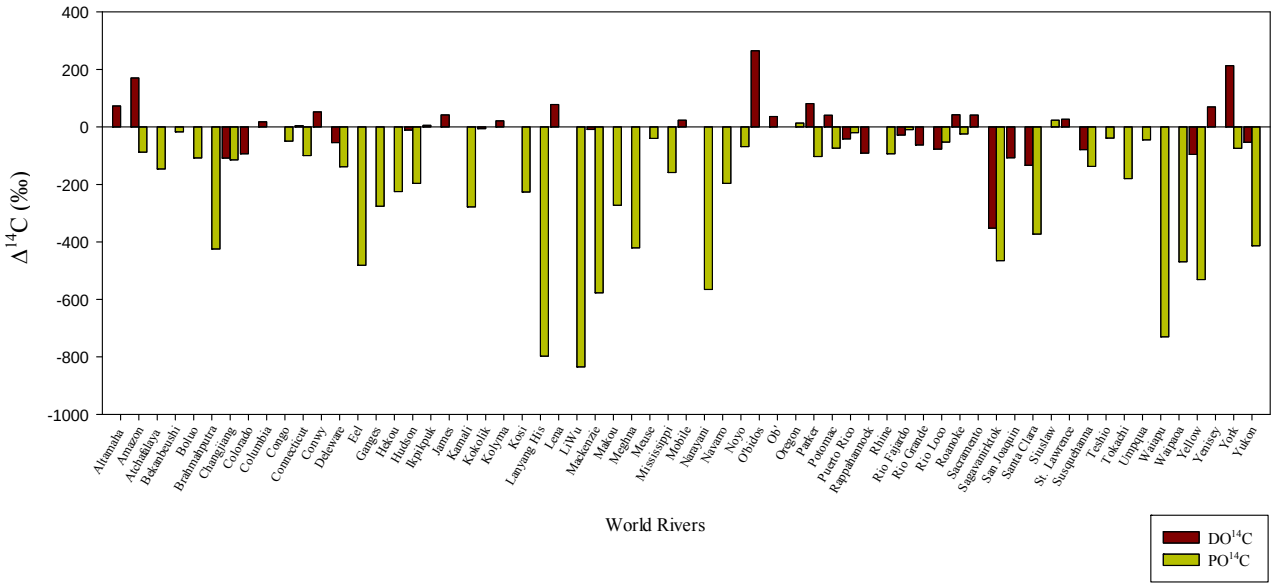

Figure 7: The $\Delta^{14}C$ values arranged in order according to proximity to the North Pole. Average values were used when available, otherwise reported value used (when only one observation).

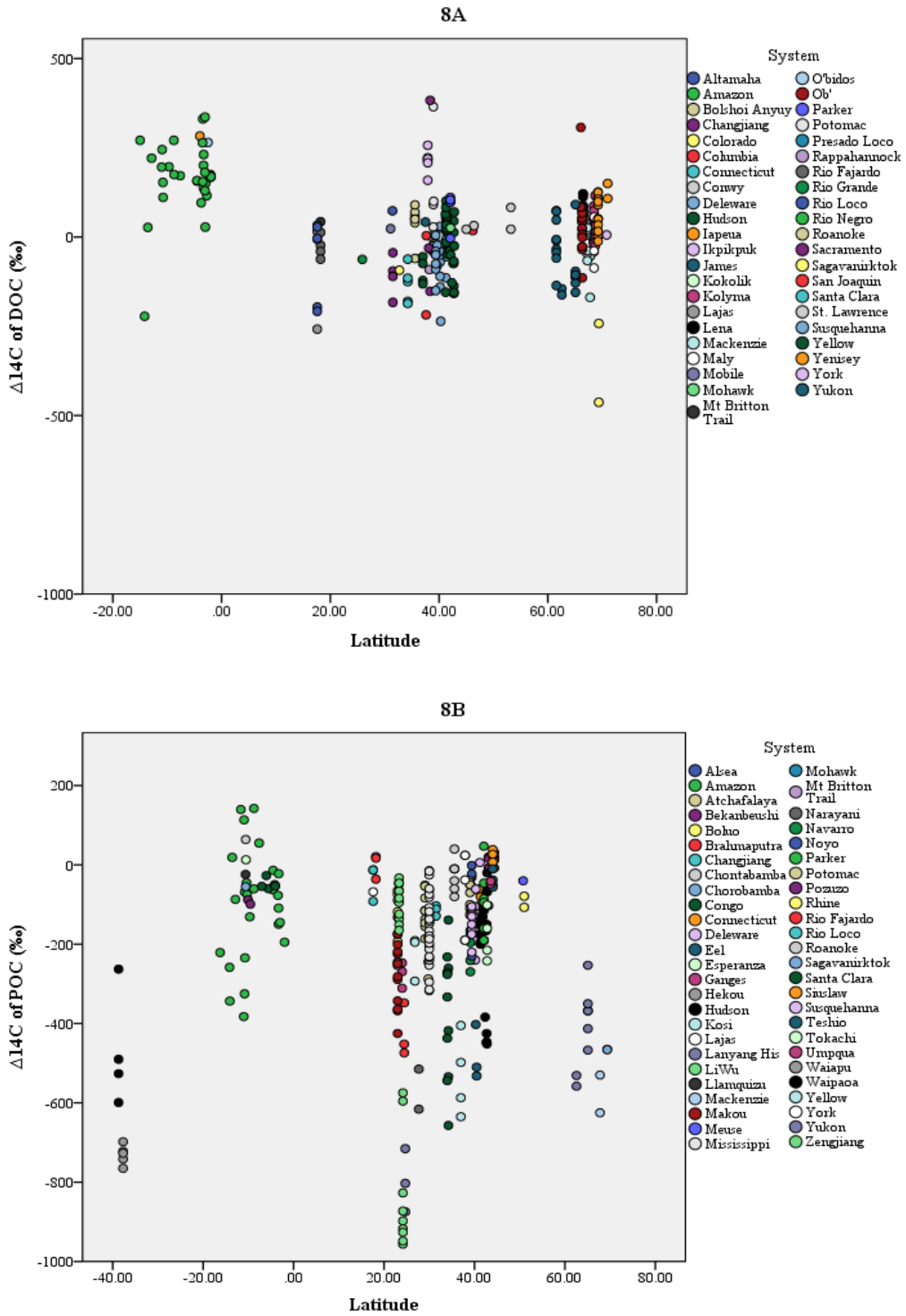

Figure 8: Individual observations for the 8A) $\Delta^{14}C$ - DOC and latitude and 8B) $\Delta^{14}C$ - POC observations and latitude for each riverine system (signified by different colors).

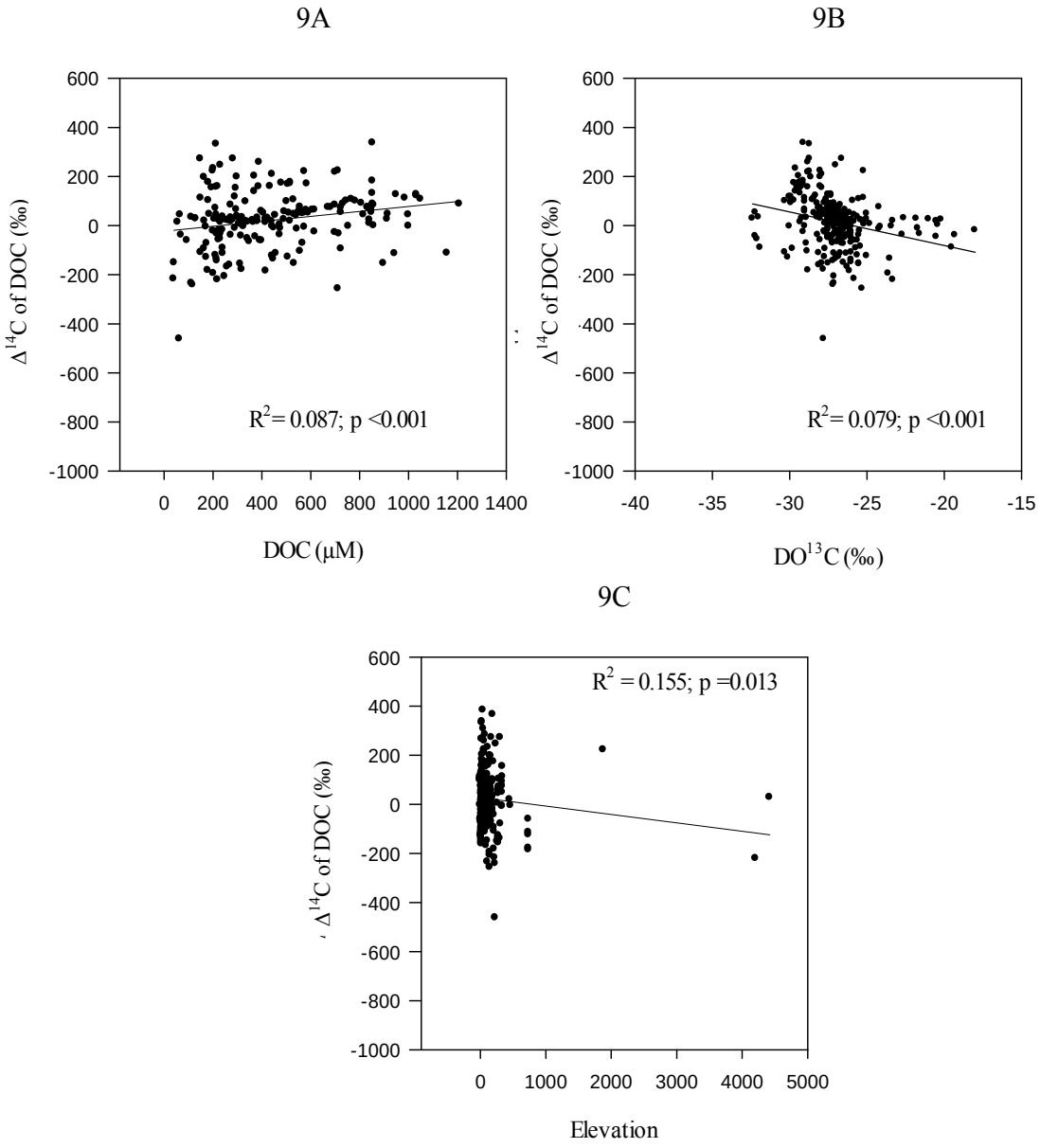

Figure 9: Regressions of significant relationships for $\Delta^{14}C$ of DOC and 9A) DOC (μM), 9B) $DO^{13}C$ (‰), and 9C) Elevation (m).

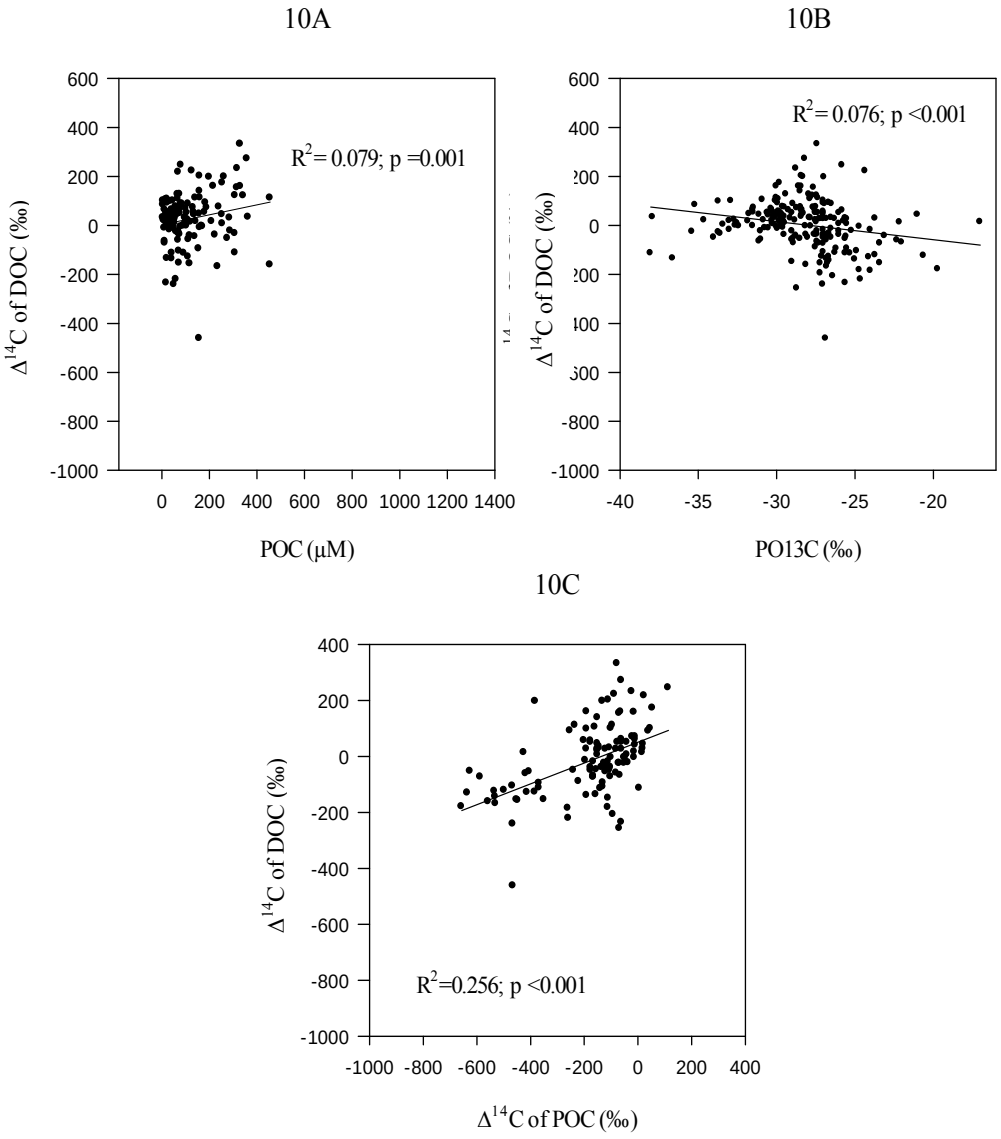

Figure 10: Regressions showing the relationship between Δ^{14}C of DOC and 10A) POC (µM), 10B) $PO^{13}C$ signature (‰), and 10C) Δ^{14}C of POC (‰)

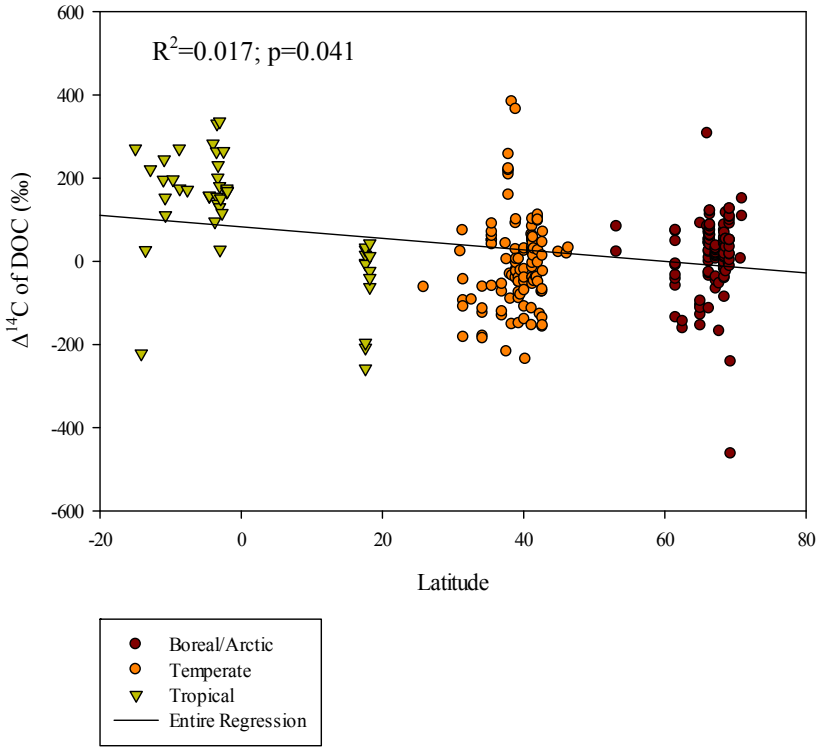

Figure 11: Linear regressions showing the relationship between the radiocarbon age of DOC and latitude for all the points. Individual regressions for each climate group are also shown (solid lines): Boreal/Arctic (R^2=0.034; p=0.053), Temperate (R^2=0.046; p=0.024) and Tropical (R^2=0.367; p<0.001).

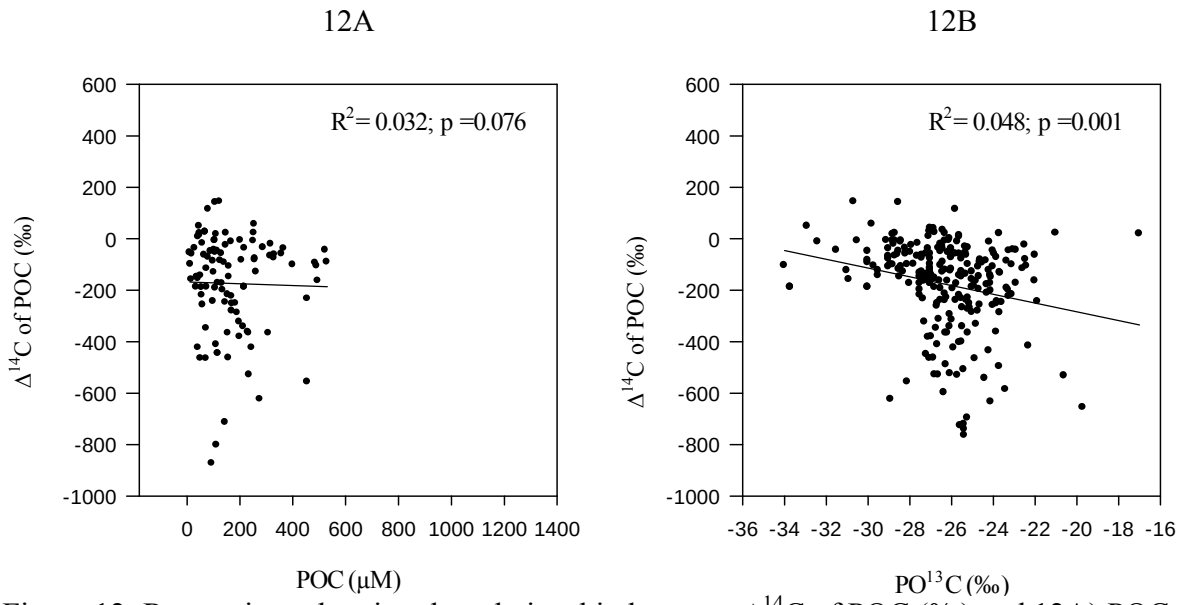

Figure 12: Regressions showing the relationship between Δ^{14}C of POC (‰) and 12A) POC concentration (µM) and 12B) PO^{13}C signature (‰)

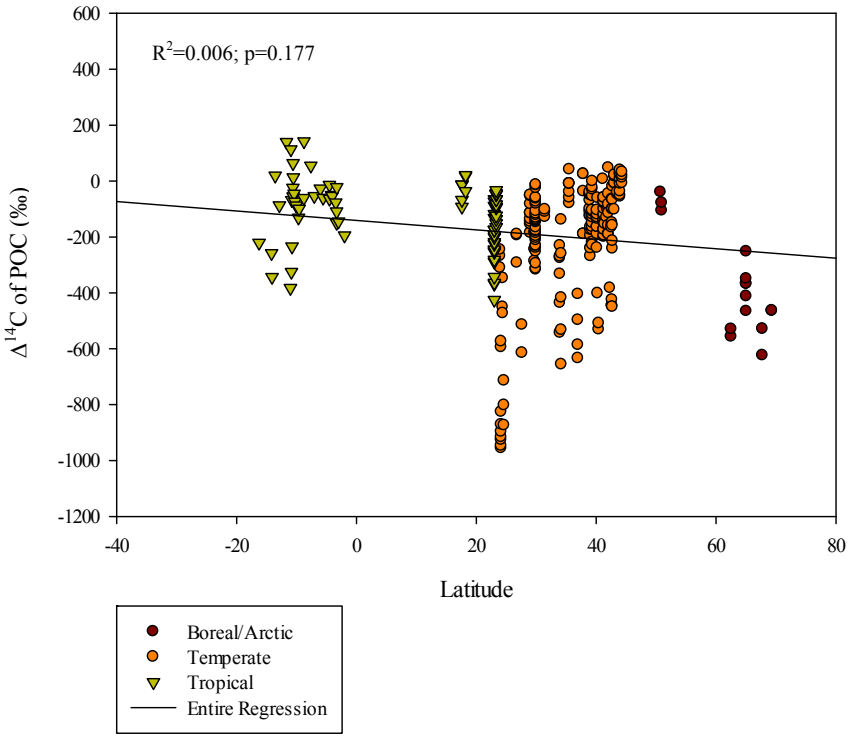

Figure 13: Linear regression for the radiocarbon age of POC and latitude. Individual examination of climate groups yield regressions for Boreal/Arctic (R^2=0.767; p<0.001), Temperate (R^2=0.279; p<0.001), and Tropical (R^2=0.050; p=0.058) (solid lines) Observations falling near 40°S (New Zealand Rivers) were not included due to vast differences from other temperate rivers.

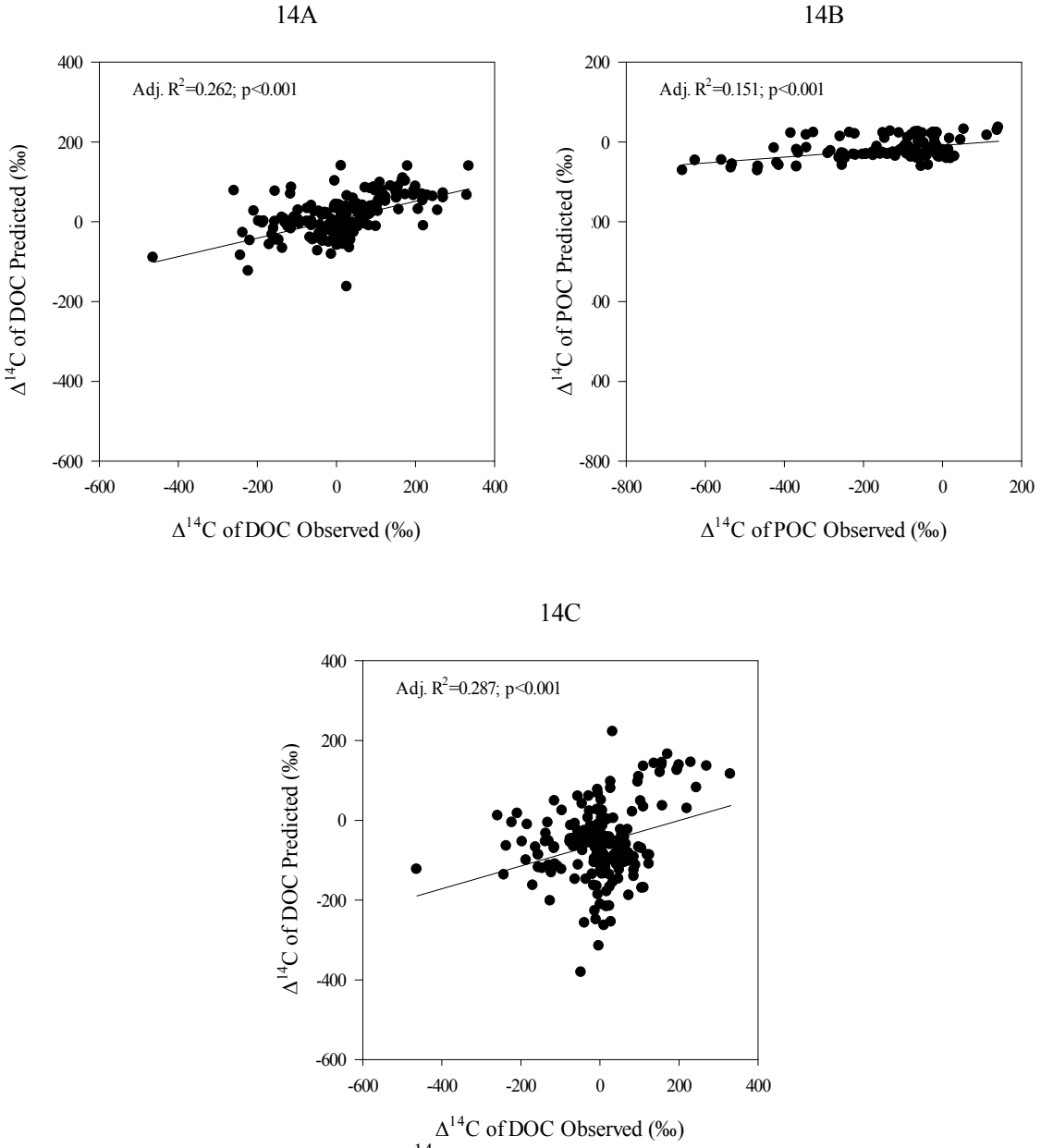

Figure 14: Relationship between $\Delta^{14}C$ and driving factors predicted by the multiple regression equation and all data maeasured. #A) $\Delta^{14}C$ DOC predicted by MLR $DO^{14}C$ ($lnDO^{14}C(age) = 8.243 – 4.53E4$ DOC (µM) + 0.017 $DO^{13}C$ (‰) + 1.26E4 Elevation + 0.005 Latitude. #B) $\Delta^{14}C$ POC predicted by MLR $PO^{14}C$ ($lnPO^{14}C(age) = 8.530 – 4.75E4$ POC (µM) + 0.040 $PO^{13}C$ (‰) + 0.007 Latitude. #C) $\Delta^{14}C$ DOC predicted by MLR $DO^{14}C/PO^{14}C$ ($lnDO^{14}C(age) = 10.895 + 0.072$ $DO^{13}C$ (‰) + 0.049 $PO^{13}C$ (‰) + 0.009 Latitude.

15A

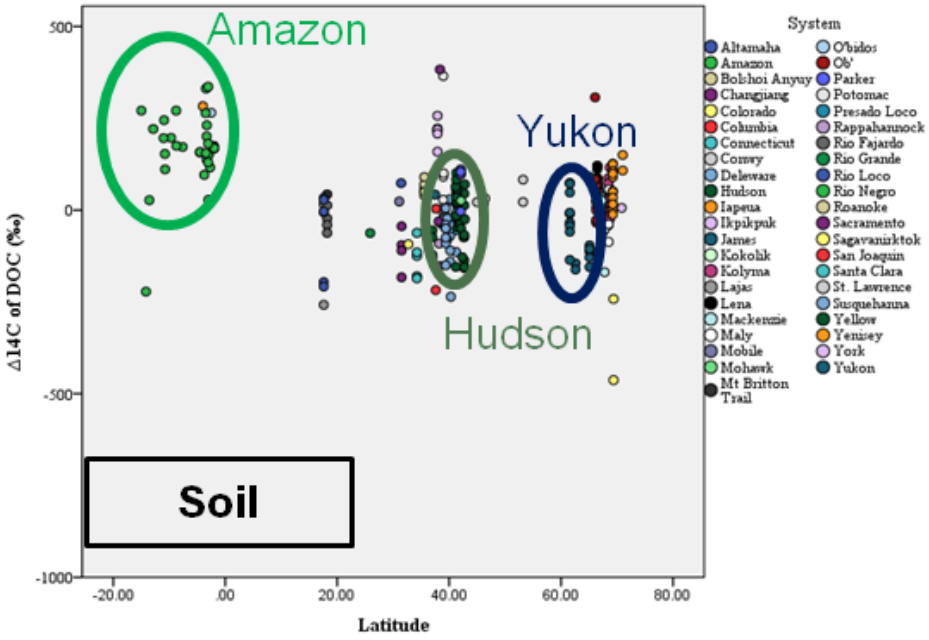

15B

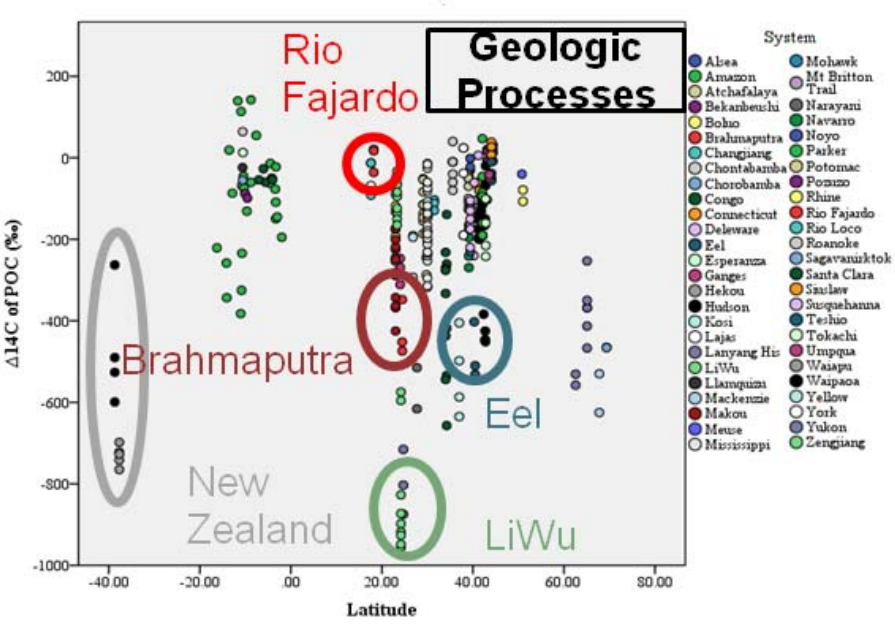

Figure 15: Variations in 15A) $\Delta^{14}C$ of DOC in systems characterized with different elevations, and in 15B) $\Delta^{14}C$ of POC in systems characterized with steep slope and rapid uplift. Circles with similar color to names of rivers correspond with one another.

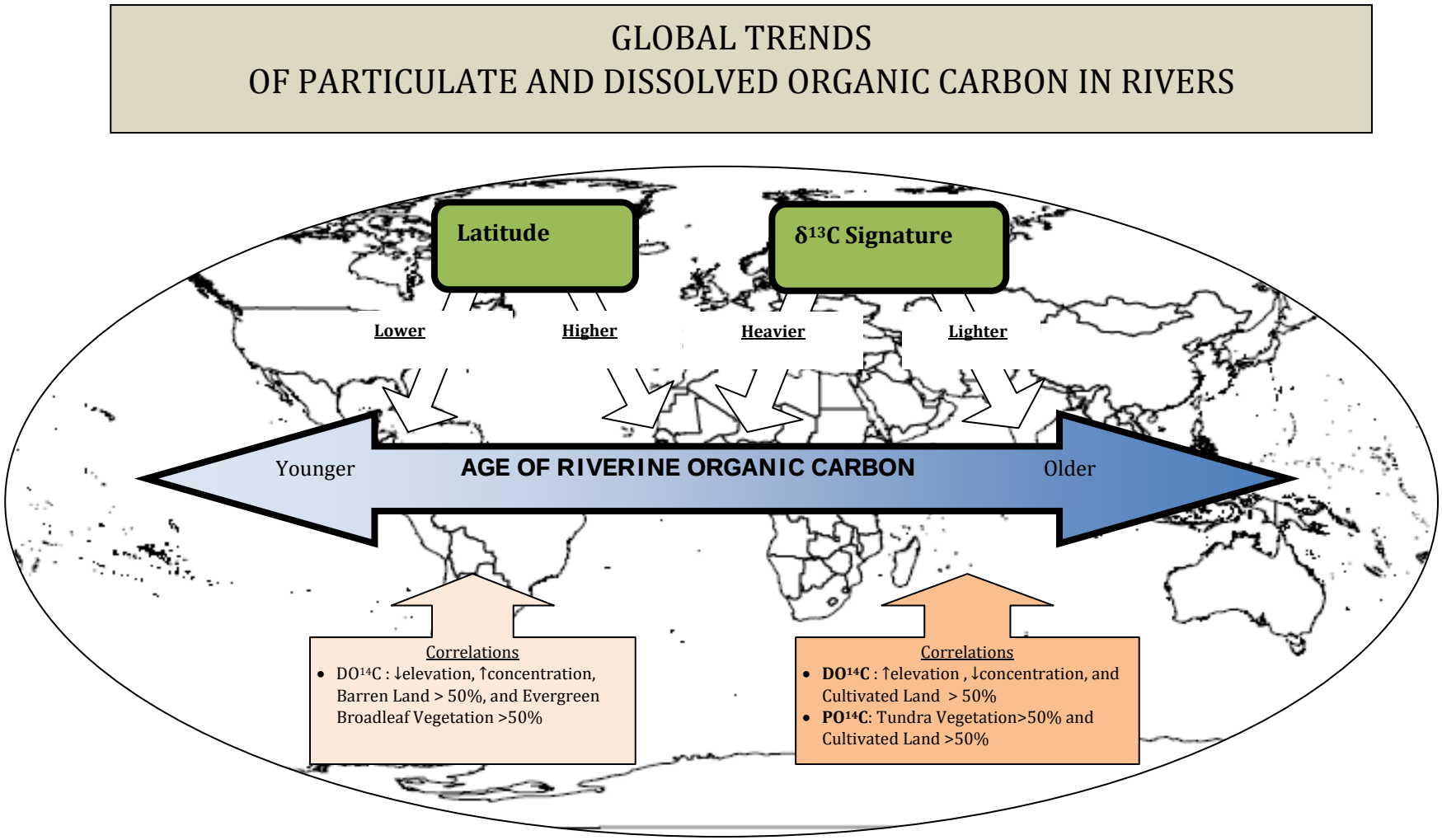

Figure 16: Conceptual drawing of the relationships between $\delta^{13}C$ and $\Delta^{14}C$ DOC and latitude including correlations for elevation, concentration, land cover, and vegetation.

VITA

Ashley Nicole Tucker received her B.S. in Environmental Studies from Virginia Commonwealth University in May 2011. While attending graduate school, she assisted with research in the Biogeochemical Lab at VCU and was a teaching assistant for Oceanography, a course offered by the Center for Environmental Studies. During her final year of graduate school, she maintained a position with the County of Henrico as a laboratory analyst at the Central Environmental Lab/Water Reclamation Facility.